



This is to certify that the
thesis entitled
Buckling of a Two-Ply
Nonlinear Elastic Plate
presented by

Yue Qiu

has been accepted towards fulfillment of the requirements for

Master's degree in Mechanics

Major professor

Date Fel 27, 1992

LIBRARY Michigan State University

PLACE IN RETURN BOX to remove this checkout from your record. TO AVOID FINES return on or before date due.

DATE DUE	DATE DUE	DATE DUE

MSU is An Affirmative Action/Equal Opportunity Institution characteristics.pm3-p.1

BUCKLING OF A TWO-PLY NONLINEAR ELASTIC PLATE

Ву

Yue Qiu

A THESIS

Submitted to
Michigan State University
in partial fulfillment of the requirements
for the degree of

MASTER OF SCIENCE

Department of Materials Science and Mechanics

ABSTRACT

BUCKLING OF A TWO-PLY NONLINEAR ELASTIC PLATE

By

Yue Qiu

The buckling of a two-ply nonlinear elastic plate is studied in the context of finite deformation incompressible nonlinear elasticity. The formulation proceeds by using the theory of superposing an incremental nonhomogeneous deformation onto a finite homogeneous deformation. Numerical procedures are then used to investigate the bifurcation and to determine the buckling stretch ratio and buckling thrust. The buckling mode is studied and it is found that the buckling deformation of the two-ply composite plate without symmetry in direction of thickness is of a mixed mode character involving both flexure and barrelling.

ACKNOWLEDGMENTS

I would like to express sincere appreciation to my advisor, Professor Thomas J. Pence for his very helpful guidance and support throughout this work. I would also like to express my special thanks to my parents and my wife. They are always my sources of encouragements.

The financial support for this work from the Research Excellence Fund for composite materials, administered by the Michigan State University Composite Materials and Structures Center, is also gratefully acknowledged.

TABLE OF CONTENTS

1.	Introduction	1
2.	Problem Formulation	4
	2.1. Problem Description	4
	2.2. Formulation	5
	2.3. Bifurcation from the Homogeneous Solution	10
3.	Solution of the Buckling Equation for Correlation of	
	Load Parameter λ with Mode Parameter η	17
	3.1. Asymptotic Analysis for Large λ	19
	3.2. Asymptotic Analysis for Large η	23
	3.3. Numerical Analysis	26
4.	Deformation	34
5.	Discussion	41
	List of References	52
	Appendix	54

1. INTRODUCTION

Buckling of load bearing plates is a major type of structural failure in which the plate reconfigures itself in such a fashion that often causes it to lose the capability of carrying loads. So this kind of problem has been of concern for a long time by numerous researchers. For example, Sawyers and Rivlin [3](1974), [4](1982) employed the theory of small deformation superposed onto finite deformation [1] to determine the critical conditions of bifurcation. These conditions are derived upon general strain energy function and their results can be applied to the determination of bifurcation conditions corresponding to any specified strain energy function. They published their extensive studies on the instability of rectangular plate of incompressible isotropic elastic material with neo-Hookean strain energy function subject to a thrust. Biot's [8](1968) study on the edge buckling of a laminated medium is another issue in this area, according to which, while the top and bottom faces of a semi-infinite laminated plate are kept from normal displacements, buckling takes place locally along the edge subject to a compressive stress. Pence and Song [9](1990), [10](1991) have published their research on the buckling instability in highly deformable composite laminate plate. They examined in detail the buckling instability of a thick rectangular three-ply sandwich composite plate with material and geometrical symmetry in direction of thickness. The plate they considered is composed of three stacked rectangular plies with perfectly interfacial bonding. These plies are made up of two different incompressible isotropic nonlinear elastic materials. The top and bottom plies are identical both in material and in thickness. The buckling instability of this plate under thrust has been extensively studied, and carried out a lot of valuable results. Unlike the noncomposite case (Sawyers and Rivlin [3], [4]), this three-ply composite case gives rise to additional families of buckled solutions. So the question arises as to how these new families of solutions are correlated with laminate number n. In order to study this question and, motivated also by the purpose of investigating the buckling behaviors corresponding to the different way the plies stacked, we carried out a study on the buckling instability of a two-ply composite plate without symmetry in direction of thickness.

Generally, in the class of problems of this type, if the plate is composed by n plies, the possibility of bifurcation requires the solution of a $4n \times 4n$ system of equations. With the symmetry in direction of thickness, the system can reduce to a $2n \times 2n$ one. There are various number of ways to stack plies, with or without symmetry. The investigation on the two-ply problem may have basic meaning. It can give a view on whether and how, to some extent, the buckling behaviors will vary with the number of plies and on the situation with or without symmetry. In this thesis, we present our studies and the results obtained on the instability of a thick rectangular nonlinear elastic composite plate made up of two plies of incompressible isotropic neo-Hookean materials under a total thrust.

In Chapter 2, the problem is described and the basic boundary value problem is formulated. The composite plate of dimensions $2l_1 \times 2l_2 \times 2l_3$ composed by two plies of incompressible neo-Hookean materials are constrained by the requirements that (1) the top and bottom faces are traction free and (2) the displacement and traction are continuous across the interface of the two plies corresponding to a perfect bonding. These give the boundary and interface conditions (2.11)-(2.13). A thrust T acts on the faces initially at $X_1 = \pm l_1$. The incompressibility condition (2.4) and the governing equation (2.10) together with (2.11)-(2.13) form a complete boundary value problem. Finally, these yield the bifurcation condition (2.67).

In Chapter 3, asymptotic analyses are conducted for the bifurcation condition. These give similar results to those obtained by Kim in his study of the three-ply problem [13]. The numerical procedure used to solve the bifurcation condition and to obtain the buckling stretch ratio and buckling thrust is described in section 3.3. The results obtained are also discussed in this chapter.

We present the investigation on deformation modes in Chapter 4. The buckling deformation of the composite plate is in mixed mode with flexural and barrelling characters. In this chapter we decompose the deformation into four parts, namely, smooth flexure, smooth barrelling, residual flexure and residual barrelling, and examine the continuity of these parts across the interface.

In the last chapter, we briefly discuss the portions of these four parts of deformations occupying a possible total deformation under thrust. We also give pictures of these decomposed deformation modes. Finally, in closing this thesis, we investigate the influence of lack of symmetry in direction of thickness on the deformation mode.

2. PROBLEM FORMULATION

Following Sawyers and Rivlin [3] [4] as well as Pence and Song [9] [10], we shall formulate the solution system for the problem by superposing an incremental non-homogeneous deformation onto a finite homogeneous deformation solution in this chapter.

2.1. PROBLEM DESCRIPTION

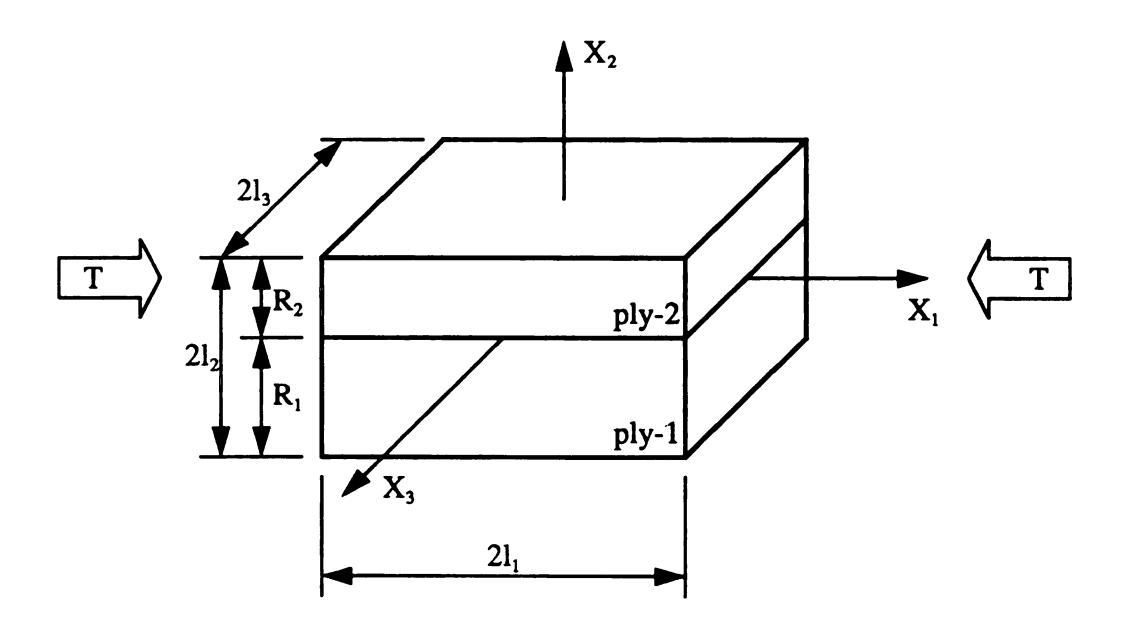


Figure 2.1. The geometrical description of a two-ply composite plate.

The geometrical description of the composite plate under consideration is shown in Figure 2.1. By setting the origin of the coordinate system at the center of the interface of the two plies, the plate occupies

$$\begin{aligned} -l_1 &\leq X_1 \leq l_{1,} \\ \text{ply-1:} & -R_1 \leq X_2 \leq 0, \qquad \text{ply-2:} & 0 \leq X_2 \leq R_{2,} \\ & -l_3 \leq X_3 \leq l_3 \end{aligned} \tag{2.1}$$

in its undeformed configuration, where R_1 is the thickness of ply-1, R_2 is the thickness of ply-2, and $R_1+R_2=2l_2$. Ply-1 and ply-2 are both of incompressible neo-Hookean

materials. But the shear moduli of ply-1 and ply-2 are different in general.

A thrust T is applied on faces initially at $X_1 = \pm l_1$. Assume that the surfaces initially at $X_2 = -R_1$ and $X_2 = R_2$ are traction free. The surfaces initially at $X_3 = \pm l_3$ are assumed to be kept from normal displacements by means of applying certain frictionless forces onto them.

2.2. Formulation

Upon loading on the composite material construction, first, a finite homogeneous deformation is taken into account, and second, linearized incremental deformations are superposed onto the homogeneous deformation following [3] [10].

The deformation within each ply is

$$\mathbf{x} = \mathbf{x}(\mathbf{X}) , \qquad (2.2)$$

and the corresponding deformation gradient tensor is expressed as

$$\mathbf{F} = \frac{\partial \mathbf{x}}{\partial \mathbf{X}}.\tag{2.3}$$

The incompressibility of the material then gives the constraint

$$det(\mathbf{F}) = 1. \tag{2.4}$$

The left Cauchy-Green strain tensor is defined as

$$\mathbf{B} = \mathbf{F}\mathbf{F}^T, \tag{2.5}$$

and its eigenvalues are denoted by λ_1^2 , λ_2^2 , λ_3^2 , which are the squares of the principal stretches λ_1 , λ_2 , λ_3 . The most general strain energy density function for an incompressible isotropic elastic material is given by

$$W = W(I_1, I_2),$$
 (2.6)

and the associated Cauchy stress tensor for a general incompressible elastic material is then given by

$$\tau = -p\mathbf{I} + 2\left(\frac{\partial \mathbf{W}}{\partial \mathbf{I}_1} + \mathbf{I}_1 \frac{\partial \mathbf{W}}{\partial \mathbf{I}_2}\right) \mathbf{B} - 2\left(\frac{\partial \mathbf{W}}{\partial \mathbf{I}_2}\right) \mathbf{B}^2, \tag{2.7}$$

where p is hydrostatic pressure and I_1 , I_2 are the first and second invariants of **B**. We further denote

$$W^{(i)} = W^{(i)} (I_1, I_2),$$

 $W^{(ii)} = W^{(ii)} (I_1, I_2),$
(2.8)

for ply-1 and ply-2 respectively. The Piola-Kirchoff stress tensor is given by

$$\mathbf{s} = \mathbf{F}^{-1} \mathbf{\tau}. \tag{2.9}$$

The equilibrium equations with the absence of body forces and inertia terms in tensor form are

$$div \mathbf{s}^T = \mathbf{0}. (2.10)$$

In the buckling problem considered, normal thrusts of magnitude T act on the two surfaces initially at $X_1 = \pm l_1$. By assumption, surfaces initially at $X_2 = -R_1$ and $X_2 = R_2$ are traction free and surfaces initially at $X_3 = \pm l_3$ are kept in the original planes. These consequently require the following boundary conditions to be satisfied:

$$s_{12} = s_{13} = 0,$$
 on $X_1 = \pm l_1;$
 $s_{21} = s_{22} = s_{23} = 0,$ on $X_2 = -R_1$ and $X_2 = R_2;$ (2.11)
 $s_{31} = s_{32} = 0,$ on $X_3 = \pm l_3;$

$$x_1 = \pm \rho l_1$$
, on $X_1 = \pm l_1$;
 $x_3 = \pm l_3$, on $X_3 = \pm l_3$. (2.12)

Here ρ is the overall imposed stretch in the X_1 direction, it shall shortly be shown that ρ is uniquely determined by the thrust T. Across the interface of the two-ply composite material, both tractions and displacements are required to be continuous. That is,

$$s_{2i}|_{X_{2}^{+}} = s_{2i}|_{X_{2}^{-}}, \quad \text{on } X_{2} = 0 \text{ (i=1,2,3);}$$

$$\mathbf{x}|_{X_{2}^{+}} = \mathbf{x}|_{X_{2}^{+}}, \quad \text{on } X_{2} = 0.$$
(2.13)

This corresponds to the assumption of a perfect bond.

The governing equation (2.10) with boundary conditions (2.11), (2.12) and (2.13) and with the incompressibility constraint (2.4) consist of a complete boundary value problem, which has exactly one pure homogeneous solution as follows:

$$x_1 = \rho X_1$$
,
 $x_2 = \rho^{-1} X_2$,
 $x_3 = X_3$, (2.14)

and so gives the principal stretches

$$\lambda_1 = \rho, \qquad \lambda_2 = \rho^{-1}, \qquad \lambda_3 = 1.$$
 (2.15)

The deformation gradient tensor (2.3) then has the form

$$\mathbf{F} = \begin{bmatrix} \rho & 0 & 0 \\ 0 & \rho^{-1} & 0 \\ 0 & 0 & 1 \end{bmatrix}, \tag{2.16}$$

and the left Cauchy-Green strain tensor (2.5) then yields

$$\mathbf{B} = \begin{bmatrix} \rho^2 & 0 & 0 \\ 0 & \rho^{-2} & 0 \\ 0 & 0 & 1 \end{bmatrix}, \tag{2.17}$$

of which the invariants are

$$I_{1} = \lambda_{1}^{2} + \lambda_{2}^{2} + \lambda_{3}^{2} = 1 + \rho^{2} + \rho^{-2},$$

$$I_{2} = \lambda_{1}^{2} \lambda_{2}^{2} + \lambda_{2}^{2} \lambda_{3}^{2} + \lambda_{3}^{2} \lambda_{1}^{2} = 1 + \rho^{2} + \rho^{-2},$$

$$I_{3} = \lambda_{1}^{2} \lambda_{2}^{2} \lambda_{3}^{2} = 1.$$
(2.18)

The incompressibility constraint (2.4) is satisfied by the homogeneous solution (2.14).

Since **F**, **B** are constant tensors, following (2.6), (2.7) and (2.9), the equilibrium equation (2.10) requires that the hydrostatic pressure p in (2.7) is individually constant in each ply, it shall be denoted by $p^{(i)}$ for ply-1 and $p^{(ii)}$ for ply-2.

The strain energy density function for a neo-Hookean material is given by

$$W = \frac{\mu(I_1 - 3)}{2}, \tag{2.19}$$

or

$$W^{(i)} = \frac{\mu^{(i)} (I_1 - 3)}{2},$$

$$W^{(ii)} = \frac{\mu^{(ii)} (I_1 - 3)}{2}$$
(2.20)

for ply-1 and ply-2 respectively.

The Cauchy stress tensor (2.7) thus yields

$$\tau = -p^{(j)} \mathbf{I} + \mu^{(j)} \mathbf{B}, \quad j = i, ii.$$
 (2.21)

By substituting (2.17) into (2.21), it yields

$$\tau = \begin{bmatrix} -p^{(j)} + \mu^{(j)} \rho^2 & 0 & 0 \\ 0 & -p^{(j)} + \mu^{(j)} \rho^{-2} & 0 \\ 0 & 0 & -p^{(j)} + \mu^{(j)} \end{bmatrix}.$$
 (2.22)

The Piola-Kirchoff stress tensor (2.9) becomes

$$\mathbf{s} = \begin{bmatrix} -\mathbf{p}^{(j)} \rho^{-1} + \boldsymbol{\mu}^{(j)} \rho & 0 & 0 \\ 0 & -\mathbf{p}^{(j)} \rho + \boldsymbol{\mu}^{(j)} \rho^{-1} & 0 \\ 0 & 0 & -\mathbf{p}^{(j)} + \boldsymbol{\mu}^{(j)} \end{bmatrix}. \tag{2.23}$$

From stress boundary conditions $(2.11)_2$, $s_{22} = 0$ gives

$$p^{(j)} = \mu^{(j)} \rho^{-2}, \quad j = i, ii.$$
 (2.24)

Substituting (2.24) into (2.22) and (2.23), τ and s become

$$\tau = \mu^{(j)} \begin{bmatrix} \rho^2 - \rho^{-2} & 0 & 0 \\ 0 & 0 & 0 \\ 0 & 0 & 1 - \rho^{-2} \end{bmatrix} \equiv \tau^{(j)}, \quad j = i, ii$$
 (2.25)

and

$$\mathbf{s} = \mu^{(j)} \begin{bmatrix} \rho - \rho^{-3} & 0 & 0 \\ 0 & 0 & 0 \\ 0 & 0 & 1 - \rho^{-2} \end{bmatrix} \equiv \mathbf{s}^{(j)}, \quad \mathbf{j} = \mathbf{i}, \mathbf{i}\mathbf{i}.$$
 (2.26)

Note that the equilibrium equation (2.10) is satisfied by (2.26) as contributed by the homogeneous solution (2.14). All the boundary conditions (2.11), (2.12) and (2.13) are satisfied by the Piola-Kirchoff stress tensor (2.26) for the pure homogeneous deformation (2.14).

Let T be the total thrust applied onto each of the surfaces $X_1 = \pm l_1$ and let $T^{(j)}$ be the portions of T applied to material j only (j = i, ii), so

$$T = T^{(i)} + T^{(ii)}$$
. (2.27)

Thus, for the homogeneous solution

$$\tau_{11}^{(j)} = -\frac{T^{(j)}}{A^{(j)}}$$
 $j = i, ii,$ (2.28)

where $A^{(j)}(j = i, ii)$ is the current area of the surface to which $T^{(j)}$ is applied,

$$A^{(i)} = 2R_1 l_3 \rho^{-1},$$

$$A^{(ii)} = 2R_2 l_3 \rho^{-1}.$$
(2.29)

Using (2.25), (2.28) and (2.29), it is obtained from (2.27) that

$$T = -2l_3 (\rho - \rho^{-3}) (\mu^{(i)} R_1 + \mu^{(ii)} R_2), \qquad (2.30)$$

or

$$T^{(i)} = -\frac{\mu^{(i)} R_1}{\mu^{(i)} R_1 + \mu^{(ii)} R_2} T,$$

$$T^{(ii)} = -\frac{\mu^{(ii)} R_2}{\mu^{(i)} R_1 + \mu^{(ii)} R_2} T.$$
(2.31)

2.3. Bifurcation From the Homogeneous Solution

The stability of the foregoing homogeneous solution for the two-ply composite plate under thrust is to be investigated from now on, using the theory of incremental deformations superposed onto finite homogeneous solution. Attention is restricted to buckling that takes place in the X_1 - X_2 plane. Let $\bf u$ be the incremental deformation that is to be superposed onto the homogeneous deformation (2.14). Then $\bf u$ has components

$$u_1 = u_1(X_1, X_2),$$

 $u_2 = u_2(X_1, X_2),$
 $u_3 = 0.$ (2.32)

The fully finite deformation $\hat{\mathbf{x}}$ can be expressed as

$$\hat{x}_{1} = \rho X_{1} + \varepsilon u_{1} (X_{1}, X_{2}),$$

$$\hat{x}_{2} = \rho^{-1} X_{2} + \varepsilon u_{2} (X_{1}, X_{2}),$$

$$\hat{x}_{3} = X_{3},$$
(2.33)

where ε is an order parameter which is used to obtain a linearized problem governing bifurcation from the homogeneous solution (2.14). Following Pence and Song [10], we use a superposed $^{\wedge}$ to indicate quantities associated with the fully finite deformation (2.33) and a superposed $^{-}$ to indicate linearized incremental quantities associated with the incremental deformations. Hence, the pressure field corresponding to (2.33) is given by

$$\hat{\mathbf{p}}(\mathbf{X}, \boldsymbol{\varepsilon}) = \mathbf{p}^{(j)} + \boldsymbol{\varepsilon} \bar{\mathbf{p}}(\mathbf{X}_1, \mathbf{X}_2, \mathbf{X}_3) + O(\boldsymbol{\varepsilon}^2), \quad j = i, ii, \quad (2.34)$$

and the Piola-Kirchoff stress tensor is given by

$$\hat{\mathbf{s}}(\mathbf{X}, \boldsymbol{\varepsilon}) = \mathbf{s}^{(j)} + \boldsymbol{\varepsilon} \bar{\mathbf{s}}(\mathbf{X}_1, \mathbf{X}_2, \mathbf{X}_3) + O(\boldsymbol{\varepsilon}^2), \qquad j = i, ii. \tag{2.35}$$

From (2.33), the deformation gradient tensor yields

$$\hat{\mathbf{F}} = \begin{bmatrix} \rho + \varepsilon \mathbf{u}_{1,1} & \varepsilon \mathbf{u}_{1,2} & 0 \\ \varepsilon \mathbf{u}_{2,1} & \rho^{-1} + \varepsilon \mathbf{u}_{2,2} & 0 \\ 0 & 0 & 1 \end{bmatrix}, \qquad (2.36)$$

its determinant is readily obtained as

$$\det \hat{\mathbf{F}} = 1 + \varepsilon (\rho \mathbf{u}_{2,2} + \rho^{-1} \mathbf{u}_{1,1}) + O(\varepsilon^2) . \tag{2.37}$$

From now on, we restrict attention to the linearized problem and omit any incremental quantities of $O(\varepsilon^2)$. The incompressibility constraint $\det \bar{\mathbf{F}} = 1$ thus gives

$$\rho u_{2,2} + \rho^{-1} u_{1,1} = 0. (2.38)$$

The inverse of $\overline{\mathbf{F}}$ is given by

$$\overline{\mathbf{F}}^{-1} = \begin{bmatrix} \rho^{-1} + \varepsilon \mathbf{u}_{2,2} & -\varepsilon \mathbf{u}_{1,2} & 0 \\ -\varepsilon \mathbf{u}_{2,1} & \rho + \varepsilon \mathbf{u}_{1,1} & 0 \\ 0 & 0 & 1 \end{bmatrix}.$$
 (2.39)

The Cauchy-Green strain tensor (see (2.5)) can then be expressed as

$$\overline{\mathbf{B}} = \begin{bmatrix} \rho^2 + 2\varepsilon\rho u_{1,1} & \varepsilon(\rho u_{2,1} + \rho^{-1} u_{1,2}) & 0\\ \varepsilon(\rho u_{2,1} + \rho^{-1} u_{1,2}) & \rho^{-2} + 2\varepsilon\rho^{-1} u_{2,2} & 0\\ 0 & 0 & 1 \end{bmatrix}.$$
 (2.40)

It follows that

$$\hat{\mathbf{s}} = -(\mathbf{p}^{(j)} + \varepsilon \bar{\mathbf{p}}) \bar{\mathbf{F}}^{-1} + \mu^{(j)} \bar{\mathbf{F}}^{-1} \bar{\mathbf{B}} \qquad j = i, ii. \tag{2.41}$$

When linearized, (2.35) becomes

$$\hat{\mathbf{s}} = \mathbf{s} + \mathbf{\varepsilon} \bar{\mathbf{s}}.\tag{2.42}$$

So, by making use of (2.24), (2.26), (2.38), (2.39) and (2.40), the linearized incremental part \bar{s} can be written as

$$\bar{\mathbf{s}} = \begin{bmatrix} -\rho^{-1}\bar{\mathbf{p}} + \mu^{(j)} (\mathbf{u}_{1,1} - \rho^{-2}\mathbf{u}_{2,2}) & \mu^{(j)} (\mathbf{u}_{2,1} + \rho^{-2}\mathbf{u}_{1,2}) & 0\\ \mu^{(j)} (\mathbf{u}_{1,2} + \rho^{-2}\mathbf{u}_{2,1}) & -\rho\bar{\mathbf{p}} + 2\mu^{(j)}\mathbf{u}_{2,2} & 0\\ 0 & 0 & -\bar{\mathbf{p}} \end{bmatrix}. \quad (2.43)$$

On account of (2.42), the governing equation becomes $div\hat{s} = divs + \varepsilon div\bar{s}$. As discussed previously in connection with (2.11)-(2.13), the equilibrium equation (2.10) and

the boundary conditions (2.11), (2.12) and (2.13) are satisfied by the stress tensor s and deformation x corresponding to the homogeneous deformation (2.14) by applying (2.24). We shall now focus on the linearized incremental boundary value problem with equilibrium equation

$$div \ \bar{\mathbf{s}} = \mathbf{0} \ , \tag{2.44}$$

and boundary conditions as in (2.11)-(2.13) are provided by substituting x with u and s with s. Equation (2.44) then yields

$$-\rho^{-1}\bar{p}_{,1} + \mu^{(j)} (u_{1,11} + u_{1,22}) = 0,$$

$$-\rho\bar{p}_{,2} + \mu^{(j)} (u_{2,22} + u_{2,11}) = 0,$$

$$-\bar{p}_{,3} = 0.$$
(2.45)

Equation (2.45)₃ can be satisfied if and only if

$$\bar{p}(X_1, X_2, X_3) = \bar{p}(X_1, X_2).$$
 (2.46)

Following Sawyers and Rivlin [3], we may obtain solutions for this problem in the form

$$u_{1} = -\sin(\Phi X_{1}) U_{1}(X_{1}),$$

$$u_{2} = \cos(\Phi X_{1}) U_{2}(X_{2}),$$

$$\bar{p} = \cos(\Phi X_{1}) P(X_{2}),$$
(2.47)

where $\Phi = k\pi/l_1$ (k = 1, 2, 3, ...), or in the form

$$u_1 = cos (\Psi X_1) U_1 (X_2),$$

 $u_2 = sin (\Psi X_1) U_2 (X_2),$
 $\bar{p} = sin (\Psi X_1) P (X_2),$
(2.48)

where $\Psi = (j-1/2)\pi/l_1$ (j = 1, 2, 3, ...). To be common, denote $\Omega = m\pi/2l_1$ (m = 2k for (2.47) and m = 2j-1 for (2.48)). Thus m is the number of half wavelength of the base deformation mode function over the length of the composite plate in the direction of the thrust T. The functions $U_1(X_2)$, $U_2(X_2)$ and $P(X_2)$ are to be determined according to the equilibrium equation (2.45) and the boundary conditions (2.11)-(2.13). By substituting either (2.47) or (2.48) into (2.45), the equilibrium equation, together with the

incompressibility constraint (2.38), gives the following set of ordinary differential equations:

$$U_{1}''(X_{2}) - \Omega^{2}U_{1}(X_{2}) - \frac{\Omega\rho^{-1}}{\mu^{(j)}}P(X_{2}) = 0,$$

$$U_{2}''(X_{2}) - \Omega^{2}U_{2}(X_{2}) - \frac{\rho}{\mu^{(j)}}P'(X_{2}) = 0,$$

$$-\rho^{-2}\Omega U_{1}(X_{2}) + U_{2}'(X_{2}) = 0,$$
(2.49)

where 'denotes differentiation with respect to X_2 . We define a new stretch ratio:

$$\lambda = \lambda_2 / \lambda_1 = \rho^{-2}. \tag{2.50}$$

By substituting (2.50) into (2.30), it becomes

$$T = 2l_3 \lambda^{-1/2} (\lambda^2 - 1) (\mu^{(i)} R_1 + \mu^{(ii)} R_2).$$
 (2.51)

The thrust T is monotone increasing in λ from $T=-\infty$ when $\lambda=0$ to $T=\infty$ when $\lambda=0$ when $\lambda=0$ when $\lambda=1$. Note that $\lambda>1$ when the composite plate is compressed in X_1 -direction and $\lambda<1$ when extended. And $\lambda=1$ when the composite plate is neither compressed nor extended. From $(2.49)_3$ we can obtain $U_1(X_2)$ from $U_2(X_2)$: $U_1(X_2)=\frac{1}{\lambda\Omega}U_2'(X_2)$. If $U_2(X_2)$ is an even (odd) function then $U_1(X_2)$ is an odd (even) function. Solving (2.49) for $U_2(X_2)$, one obtains a single fourth order ordinary differential equation

$$U_2'''' - (1 + \lambda^2) \Omega^2 U_2'' + \lambda^2 \Omega^4 U_2 = 0, \qquad (2.52)$$

and its characteristic equation

$$q^4 - (1 + \lambda^2) \Omega^2 q^2 + \lambda^2 \Omega^4 = 0$$
 (2.53)

has four real roots $\pm \Omega$, $\pm \lambda \Omega$ which yields a set (A) of four base solution functions

$$A = \{e^{\Omega X_2}, e^{-\Omega X_2}, e^{\lambda \Omega X_2}, e^{-\lambda \Omega X_2}\}. \tag{2.54}$$

The general solution of equation (2.52) can be any linear combination of the four base

solution function in set A. For the purpose of convenience in discussion, we express the general solution in equivalent hyperbolic form

$$\begin{aligned} \mathbf{U}_{2}\left(\mathbf{X}_{2}\right) &= \mathbf{L}_{1}\left(\mathbf{X}_{2}\right) cosh\left(\Omega \mathbf{X}_{2}\right) + \mathbf{L}_{2}\left(\mathbf{X}_{2}\right) sinh\left(\Omega \mathbf{X}_{2}\right) \\ &+ \mathbf{M}_{1}\left(\mathbf{X}_{2}\right) cosh\left(\lambda \Omega \mathbf{X}_{2}\right) + \mathbf{M}_{2}\left(\mathbf{X}_{2}\right) sinh\left(\lambda \Omega \mathbf{X}_{2}\right). \end{aligned} \tag{2.55}$$

Where $L_1(X_2)$, $L_2(X_2)$, $M_1(X_2)$ and $M_2(X_2)$ are step functions which are individually constant in ply-1 and ply-2 respectively and are denoted as

$$L_{n}(X_{2}) = \begin{cases} L_{n}^{(1)}, & M_{n}(X_{2}) = \begin{cases} M_{n}^{(1)}, & -R_{1} \leq X_{2} \leq 0 \\ M_{n}^{(2)}, & 0 \leq X_{2} \leq R_{2} \end{cases},$$
 (2.56)

where n = 1, 2.

The boundary conditions (2.11), (2.12) and interface conditions (2.13), expressed in terms of $U_2(X_2)$, become

$$(\lambda\Omega)^{2}U_{2}(X_{2}) + U_{2}''(X_{2}) = 0,$$

$$(\lambda\Omega)^{2}(2+1/\lambda^{2})U_{2}' - U_{2}'''(X_{2}) = 0,$$

$$on X_{2} = -R_{1} and X_{2} = R_{2};$$
(2.57)

$$U_{2}(X_{2^{*}}) = U_{2}(X_{2^{*}}),$$

$$U_{2}'(X_{2^{*}}) = U_{2}'(X_{2^{*}}),$$
on $X_{2} = 0;$
(2.58)

$$\begin{split} \mu^{(i)} \Big[\left(\lambda \Omega \right)^{2} U_{2}(X_{2^{+}}) + U_{2}''(X_{2^{+}}) \Big] \\ = & \mu^{(ii)} \Big[\left(\lambda \Omega \right)^{2} U_{2}(X_{2^{-}}) + U_{2}''(X_{2^{-}}) \Big], \\ & \text{on } X_{2} = 0. \end{split} \tag{2.59} \\ \mu^{(i)} \Big[\left(2 + 1/\lambda^{2} \right) \left(\lambda \Omega \right)^{2} U_{2}'(X_{2^{+}}) - U_{2}'''(X_{2^{+}}) \Big] \\ = & \mu^{(ii)} \Big[\left(2 + 1/\lambda^{2} \right) \left(\lambda \Omega \right)^{2} U_{2}'(X_{2^{-}}) - U_{2}'''(X_{2^{-}}) \Big], \end{split}$$

The requirement that (2.55) obeys the conditions (2.57)-(2.59) gives rise to a 8×8 linear system for 8 unknown constants denoted by the L's and M's. This system shall be written as

$$\mathbf{J_{8 \times 8} I_{8 \times 1}} = \mathbf{0_{8 \times 1}},\tag{2.60}$$

where

$$\mathbf{I} = \{L_1^{(1)}, L_2^{(1)}, M_1^{(1)}, M_2^{(1)}, L_1^{(2)}, L_2^{(2)}, M_1^{(2)}, M_2^{(2)}\}^T,$$
(2.61)

and **J** is a 8×8 matrix derived from (2.57)-(2.59), which when written in full is

$$\mathbf{J} = \begin{bmatrix} \Lambda C_1 & -\Lambda S_1 & 2\lambda C_3 & -2\lambda S_3 & 0 & 0 & 0 & 0 \\ -2S_1 & 2C_1 & -\Lambda S_3 & \Lambda C_3 & 0 & 0 & 0 & 0 \\ 1 & 0 & 1 & 0 & -1 & 0 & -1 & 0 \\ 0 & 1 & 0 & \lambda & 0 & -1 & 0 & -\lambda \\ -\Lambda & 0 & -2\lambda & 0 & \beta\Lambda & 0 & 2\beta\lambda & 0 \\ 0 & -2 & 0 & -\Lambda & 0 & 2\beta & 0 & \beta\Lambda \\ 0 & 0 & 0 & 0 & \Lambda C_2 & \Lambda S_2 & 2\lambda C_4 & 2\lambda S_4 \\ 0 & 0 & 0 & 0 & 2S_2 & 2C_2 & \Lambda S_4 & \Lambda C_4 \end{bmatrix}, \quad (2.62)$$

where
$$C_1 = cosh(\eta\alpha),$$
 $S_1 = sinh(\eta\alpha),$ $C_2 = cosh(\eta(1-\alpha)),$ $S_2 = sinh(\eta(1-\alpha)),$ $C_3 = cosh(\lambda\eta\alpha),$ $S_3 = sinh(\lambda\eta\alpha),$ $C_4 = cosh(\lambda\eta(1-\alpha)),$ $S_4 = sinh(\lambda\eta(1-\alpha)),$ $\Lambda = \lambda + 1/\lambda.$

Here we have three parameters: η , β , α , in accompany with λ , whose respective ranges are

$$\lambda > 0$$
, $\eta > 0$, $\beta > 0$, $0 \le \alpha \le 1$. (2.63)

(1) The mode number $\eta = 2\Omega l_2 = m\pi l_2/l_1$ is a dimensionless parameter scaling the buckled configuration with respect to the aspect ratio l_2/l_1 . (2) The stiffness ratio $\beta = \mu^{(ii)} / \mu^{(i)}$ is the ratio of the shear modulus of ply-2 to that of ply-1. (3) The volume fraction $\alpha = R_1/2l_2$, is the ratio of the thickness of ply-1 to the thickness of the composite plate, and so gives that the ratio of the thickness of ply-2 to the thickness of the composite plate is $R_2/2l_2=1-\alpha$. A pair of material parameters (α, β) , together with l_1 , l_2 and l_3 specifies a certain material construction. Note that, by the nature of the problem we are dealing with, a pair of (α, β) represents the same material construction as the pair (1-

 $\alpha, 1/\beta$) does.

If the material parameters (α, β) take the following values

$$\beta = 1 \text{ or } \alpha = 0 \text{ or } \alpha = 1, \tag{2.64}$$

the problem considered reduces to the noncomposite one as studied extensively by Sawyers and Rivlin [3] [4]. On the other hand, all true composite cases can be restricted by $\beta \neq 1$ and $0 < \alpha < 1$.

Bifurcation takes place provided that a nontrivial solution exists for (2.60). This requires that

$$det \mathbf{J} = 0. \tag{2.65}$$

det J is a function of λ , η , β and α , and we shall express it as

$$det \mathbf{J} = \Psi(\alpha, \beta, \eta, \lambda). \tag{2.66}$$

The necessary and sufficient condition for bifurcation to take place (2.65) then can be written as

$$\Psi(\lambda, \eta, \beta, \alpha) = 0. \tag{2.67}$$

If $\lambda=1$, it is readily seen from (2.62) that $\Lambda=2$, $C_1=C_3$, $S_1=S_3$, so that the first and the third columns of **J** are identical. Thus

$$\Psi(1, \eta, \beta, \alpha) \equiv 0. \tag{2.68}$$

So $(\lambda-1)$ must be a factor of $\Psi(\lambda,\eta,\beta,\alpha)$. Since $\lambda=1$ $(\lambda=\rho^{-2})$ gives zero thrust T, no deformation or buckling takes place, and so this inherently uninteresting case will not be considered further.

3. SOLUTION OF THE BUCKLING EQUATION FOR CORRELATION OF LOAD PARAMETERS λ WITH MODE PARAMETER η

When expanded, $\Psi(\lambda,\eta,\beta,\alpha)$ is the sum of 25 products of exponents and polynomials:

$$\Psi(\lambda, \eta, \beta, \alpha) = \frac{1}{16} \sum_{i=-12}^{12} e^{\eta \kappa_i(\lambda, \alpha)} P_i(\lambda, \beta) , \qquad (3.1)$$

where $\kappa_i = \kappa_i(\lambda, \alpha)$ are given by

$$\kappa_{0} = 0, \qquad (3.2)$$

$$\kappa_{1} = (\lambda + 1), \qquad \kappa_{-1} = -(\lambda + 1), \qquad \kappa_{-2} = -(\lambda + 2\alpha - 1), \qquad \kappa_{-3} = -(\lambda - 2\alpha + 1), \qquad \kappa_{-3} = -(\lambda - 2\alpha + 1), \qquad \kappa_{-4} = -(\lambda - 1), \qquad \kappa_{-5} = -(2\alpha\lambda - \lambda + 1), \qquad \kappa_{-6} = -(\lambda + 1)(2\alpha - 1), \qquad \kappa_{-6} = -(\lambda + 1)(2\alpha - 1), \qquad \kappa_{-7} = -(\lambda - 1)(2\alpha - 1), \qquad \kappa_{-7} = -(\lambda - 1)(2\alpha - 1), \qquad \kappa_{-8} = -(2\alpha\lambda - \lambda - 1), \qquad \kappa_{-9} = -(\lambda + 1)\alpha, \qquad \kappa_{-9} = -(\lambda + 1)\alpha, \qquad \kappa_{-10} = -(\lambda - 1)\alpha, \qquad \kappa_{-11} = -(\lambda + 1)(1 - \alpha), \qquad \kappa_{-12} = -(\lambda - 1)(1 - \alpha).$$

The $P_i(\lambda,\beta)$ are polynomials in λ and β , each of which is of the form

$$P_{i}(\lambda, \beta) = \sum_{j=-6}^{7} P_{i,j}(\beta) \lambda^{j}, \qquad (3.3)$$

(the "," does not denote differentiation). For example:

$$\begin{split} P_1\left(\lambda,\beta\right) &= (\beta-1)^2\lambda^7 - (13\beta^2 - 22\beta + 13)\,\lambda^6 \\ &+ (66\beta^2 - 100\beta + 66)\,\lambda^5 - (166\beta^2 - 260\beta + 166)\,\lambda^4 \\ &+ 223\,(\beta-1)^2\lambda^3 - (183\beta^2 - 498\beta + 183)\,\lambda^2 \\ &+ (140\beta^2 - 334\beta + 140)\,\lambda^1 - (116\beta^2 - 184\beta + 116) \\ &+ 63\,(\beta-1)^2\lambda^{-1} - (27\beta^2 - 58\beta + 27)\,\lambda^{-2} \\ &+ (18\beta^2 - 4\beta + 18)\,\lambda^{-3} - (6\beta^2 - 4\beta + 6)\,\lambda^{-4} \\ &+ (\beta-1)^2\lambda^{-5} - (\beta+1)^2\lambda^{-6} \\ &= \sum_{j=-6}^7 P_{1,\,j}(\beta)\,\lambda^j, \end{split}$$

and

$$P_{2}(\lambda, \beta) = -(\beta - 1)^{2}\lambda^{7} - 3(\beta^{2} - 1)\lambda^{6} + 14(\beta - 1)^{2}\lambda^{5}$$

$$+38(\beta^{2} - 1)\lambda^{4} - 31(\beta - 1)^{2}\lambda^{3} - 41(\beta^{2} - 1)\lambda^{2}$$

$$+20(\beta - 1)^{2}\lambda^{1} - 12(\beta^{2} - 1) + (\beta - 1)^{2}\lambda^{-1}$$

$$+11(\beta^{2} - 1)\lambda^{-2} - 2(\beta - 1)^{2}\lambda^{-3} + 6(\beta^{2} - 1)\lambda^{-4}$$

$$-(\beta - 1)^{2}\lambda^{-5} + (\beta^{2} - 1)\lambda^{-6}$$

$$= \sum_{j=-6}^{7} P_{2,j}(\beta)\lambda^{j}.$$
(3.5)

In general, it is found that

$$P_{i,j}(\beta) = P_{-i,j}(\beta),$$
 (3.6)

for i=1,2, ..., 12 and j=-6, -5, ..., 0, 1, 2, ..., 7. This gives

$$P_{i}(\lambda, \beta) = \sum_{j=-6}^{7} P_{i,j}(\beta) \lambda^{j} = \sum_{j=-6}^{7} P_{-i,j}(\beta) \lambda^{j} = P_{-i}(\lambda, \beta) . \qquad (3.7)$$

Note that (3.7) in conjunction with $\kappa_i(\lambda,\alpha) = -\kappa_i(\lambda,\alpha)$ and $\kappa_0(\lambda,\alpha) = 0$ indicates that (3.1) can also be written as

$$\Psi(\lambda, \eta, \beta, \alpha) = \frac{1}{16} P_0(\lambda, \beta) + \frac{1}{8} \sum_{i=1}^{12} \cosh(\eta \kappa_i(\lambda, \alpha)) P_i(\lambda, \beta).$$
 (3.8)

A systematic study, detailed in the Appendix, uncovers various other relations among the $P_{i,j}(\beta)$'s indicating that there are 31 "distinctive forms" from among the 350 (350 = 25 × 14) $P_{i,j}(\beta)$'s (i=-12, -11, ..., 0, ..., 11, 12; j=-6, -5, ..., 0, ..., 6, 7). In addition, it is shown in the Appendix that $\Psi(\lambda,\eta,\beta,\alpha)$ can be expressed as

$$\Psi(\lambda, \eta, \beta, \alpha) = \frac{1}{16} \Lambda^T \mathbf{P}^T \mathbf{E}, \qquad (3.9)$$

where

$$\Lambda_{14 \times 1} = [\lambda^{-6}, \lambda^{-5}, \dots, \lambda^{0}, \dots, \lambda^{6}, \lambda^{7}]^{T},$$
 (3.10)

$$\mathbf{E}_{25\times1} = \mathbf{E}(\lambda, \eta, \alpha) = \left[e^{\eta \kappa_{-12}}, e^{\eta \kappa_{-11}}, \dots, e^{\eta \kappa_0}, \dots, e^{\eta \kappa_{11}}, e^{\eta \kappa_{12}}\right]^T, \quad (3.11)$$

and $P_{25\times14}$ has entries $P_{i,j}(\beta)$, which have the property that

$$\sum_{i=-12}^{12} P_{i,j}(\beta) = 0 \qquad j = -6, -5, \dots, 7.$$
 (3.12)

In this chapter we conduct an asymptotic analysis of $\Psi(\lambda,\eta,\beta,\alpha)$ both for large λ and for large η . Then we use a numerical approach to obtain the roots of $\Psi(\lambda,\eta,\beta,\alpha)$.

3.1. Asymptotic Analysis for large λ

If λ tends to infinity while other parameters η , β and α are held fixed, then, since $0 \le \alpha \le 1$, gives $-1 \le 2\alpha - 1 \le 1$, it follows from (3.1), (3.2), (3.3) that

$$\Psi(\lambda, \eta, \beta, \alpha) = \omega(\eta, \beta, \alpha) e^{\eta \lambda} \lambda^7 + O(e^{\eta \lambda} \lambda^7), \qquad (3.13)$$

provided that $\omega(\eta, \beta, \alpha) \neq 0$. An examination of (3.2) and (3.3) gives that

$$\omega(\eta, \beta, \alpha) = \frac{1}{16} \left[e^{\eta} P_{1,7}(\beta) + e^{(2\alpha - 1)\eta} P_{2,7}(\beta) \right] + e^{(-2\alpha + 1)} P_{3,7}(\beta) + e^{-\eta} P_{4,7}(\beta).$$
(3.14)

For true composite material constructions ($0<\alpha<1$, $-1<2\alpha-1<1$), this yields

$$\omega(\eta, \beta, \alpha) = \frac{1}{4} (1 - \beta)^2 \sinh(\eta \alpha) \sinh[\eta (1 - \alpha)], \qquad (3.15)$$

because of $P_{1,7} = -P_{2,7} = -P_{3,7} = P_{4,7} = (1-\beta)^2$. In view of $\eta > 0$, $\beta > 0$ and $0 < \alpha < 1$, it follows that $\omega(\eta, \beta, \alpha) = 0$ only if $\beta = 1$. However, according to (2.64), this is also a noncomposite material construction. Thus $\omega(\eta, \beta, \alpha) \neq 0$ for true composite material constructions.

Following (3.9)-(3.12), if η =0, then

$$\mathbf{E}_{25 \times 1}(\lambda, 0, \alpha) = [1, 1, ..., 1]^T,$$
 (3.16)

which gives

$$\mathbf{P}^{T}\mathbf{E} = \left\{ \sum_{i=-12}^{12} \mathbf{P}_{i,j}(\beta) \right\} = \mathbf{0} \qquad j = -6, ..., 7,$$
(3.17)

so that (3.9) gives

$$\Psi(\lambda, 0, \beta, \alpha) \equiv 0. \tag{3.18}$$

From the definition of η that $\eta = m\pi (l_2/l_1)$, $\eta = 0$ is the extreme case that the composite plate under thrust has no thickness so that any thrust (λ) can cause buckling.

A numerical study of $\Psi(\lambda,\eta,\beta,\alpha)$ reveals that its magnitude grows extremely quickly and its sign changes sharply at locations of its roots, especially as λ or η gets large. With above restrictions, we can plot curves of $\Psi(\lambda,\eta,\beta,\alpha)/(\omega(\eta,\beta,\alpha)e^{\eta\lambda}\lambda^7)$ vs λ with given η , β and α as in figure 3.1 and figure 3.2. This gives the advantage of scaling these curves into observable graphs. Since $\omega(\eta,\beta,\alpha)e^{\eta\lambda}\lambda^7\neq 0$ whenever

 $\lambda>0$, $\eta>0$, $\beta\neq 1$ and $0<\alpha<1$, it follows that

$$\Psi(\lambda, \eta, \beta, \alpha) / (\omega(\eta, \beta, \alpha) e^{\eta \lambda} \lambda^{7}) = 0, \qquad (3.19)$$

if and only if equation (2.67) is satisfied.

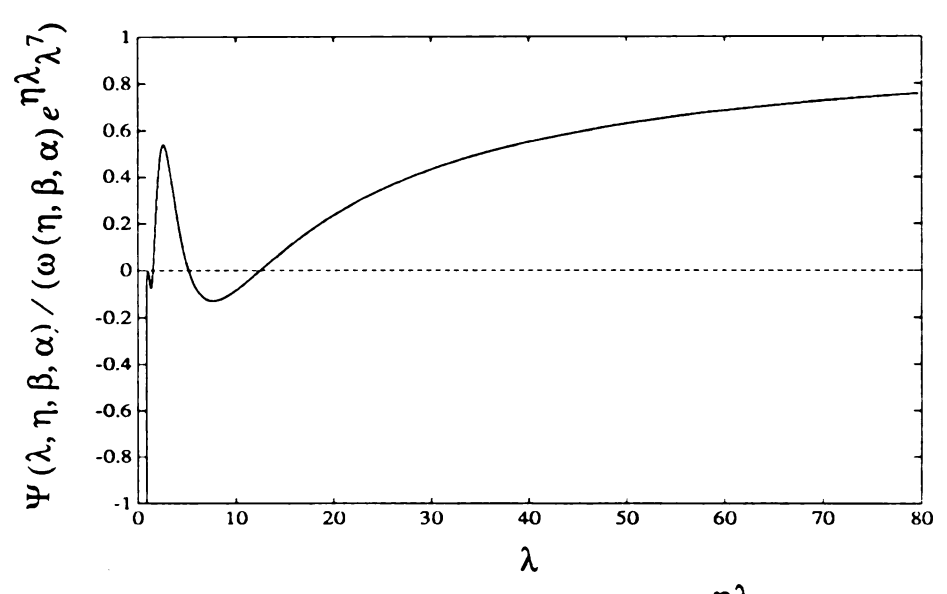


Figure 3.1. The curve of $\Psi(\lambda,\eta,\beta,\alpha)/(\omega(\eta,\beta,\alpha)e^{\eta\lambda}\lambda^7)$ vs. λ at η =2, β =3, α =0.5.

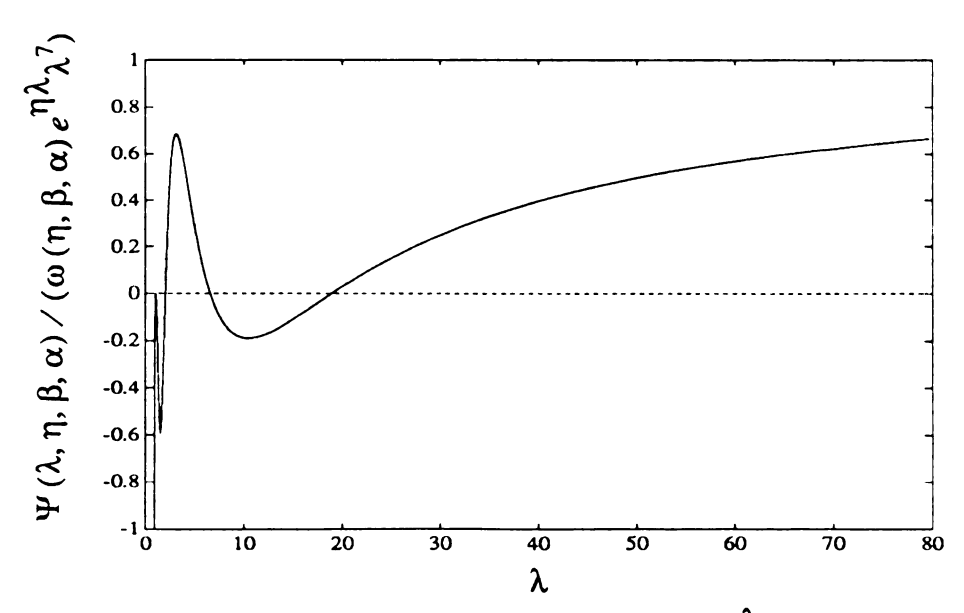


Figure 3.2. The curve of $\Psi(\lambda,\eta,\beta,\alpha)/(\omega(\eta,\beta,\alpha)e^{\eta\lambda}\lambda^7)$ vs. λ at $\eta=2,\ \beta=2,\ \alpha=0.25.$

All of the curves that have been so plotted show that the graph of $\Psi(\lambda,\eta,\beta,\alpha)$ has exactly three transversal intersection points with the line Ψ =0. All three of these intersection points are greater than one and vary continuously with η , β , α . They shall be denoted by

$$1 < \lambda_{(1)} < \lambda_{(2)} < \lambda_{(3)} \tag{3.20}$$

In addition $\lambda=1$ is also a root of (3.19) but it is not a transversal intersection, instead the graph of $\Psi(\lambda,\eta,\beta,\alpha)$ is tangent to the line $\Psi=0$ at $\lambda=1$. Finally, as expected from (3.13), note that the graph of $\Psi(\lambda,\eta,\beta,\alpha)/(\omega(\eta,\beta,\alpha)e^{\eta\lambda}\lambda^7)$ tends to one as λ tends to infinity.

It follows from (3.1) or (3.8) that the partial derivatives with respect to λ , η , β or α : $\frac{\partial \Psi}{\partial \lambda}$, $\frac{\partial \Psi}{\partial \eta}$, $\frac{\partial \Psi}{\partial \beta}$, $\frac{\partial \Psi}{\partial \alpha}$, exist and are continuous. The curves of $\Psi(\lambda, \eta, \beta, \alpha)$ /

 $(\omega(\eta,\beta,\alpha)e^{\eta\lambda}\lambda^7)$ vs. λ reveal that, for any of the three real roots $\lambda_{(i)}>1$ (i=1, 2, 3),

$$\frac{\partial}{\partial \lambda} \Psi \left(\lambda_{(i)}, \eta, \beta, \alpha \right) \neq 0. \tag{3.21}$$

Hence $\Psi(\lambda_{(i)}, \eta, \beta, \alpha) = 0$ defines three single value implicit functions

$$\lambda_{(1)} \, = \, \Phi_{1} \, (\eta, \, \beta, \, \alpha) \, , \qquad \lambda_{(2)} \, = \, \Phi_{2} \, (\eta, \, \beta, \, \alpha) \, , \qquad \lambda_{(3)} \, = \, \Phi_{3} \, (\eta, \, \beta, \, \alpha) \, \qquad (3.22)$$

respectively, such that

$$1 < \Phi_1(\eta, \beta, \alpha) < \Phi_2(\eta, \beta, \alpha) < \Phi_3(\eta, \beta, \alpha). \tag{3.23}$$

Considering the nature of $\Psi(\lambda,\eta,\beta,\alpha)$ as given in (3.1) or (3.8), it is difficult to obtain explicit expressions for $\Phi_i(\eta,\beta,\alpha)$ (i=1,2,3). Thus we employ a numerical procedure to find the functions $\Phi_i(\eta,\beta,\alpha)$ and so construct the curve presentations ($\lambda_{(i)}$ vs. η) for given (β , α). Figure 3.5-figure 3.11 are examples of these $\lambda_{(i)}$ vs. η curves with several material parameter pairs (β , α). The numerical procedure utilized will be discussed in section 3.3.

For noncomposite material constructions ($\beta=1$, $\alpha=0$ or $\alpha=1$), since $e^{\eta\lambda}\lambda^7 \neq 0$, similarly by plotting $\Psi(\lambda,\eta,\beta,\alpha)/e^{\eta\lambda}\lambda^7$ vs. λ , it is shown that there are two real roots $\lambda_{(2)}>\lambda_{(1)}>1$. These give two implicit functions of

$$\lambda_{(1)} = \Phi_1(\eta, \beta, \alpha), \qquad \lambda_{(2)} = \Phi_2(\eta, \beta, \alpha)$$
 (3.24)

in addition to the trivial root $\lambda=1$.

It is found, by using the numerical procedure (Section. 3.3), (returning to the composite material), that

$$\lim_{\eta \to 0} \Phi_{1}(\eta, \beta, \alpha) = 1,$$

$$\lim_{\eta \to 0} \Phi_{2}(\eta, \beta, \alpha) = \infty,$$

$$\lim_{\eta \to 0} \Phi_{3}(\eta, \beta, \alpha) = \infty.$$
(3.25)

3.2. Asymptotic Analysis for large η

Since $0 \le \alpha \le 1$, it follows that $-1 \le 2\alpha - 1 \le 1$, which, since $\lambda > 0$, gives (referring to (3.2))

$$\kappa_1 = max(\kappa_{-12}, \kappa_{-11}, ..., \kappa_0, ..., \kappa_{11}, \kappa_{12})$$
(3.26)

Hence

$$\Psi(\lambda, \eta, \beta, \alpha) \sim e^{\eta(\lambda+1)} P_1(\lambda, \beta)$$
 as $\eta \to \infty$. (3.27)

Since $e^{\eta(\lambda+1)} \neq 0$, it follows that solutions of

$$P_1(\lambda, \beta) = 0 \tag{3.28}$$

yields asymptotic solutions to (2.67) as $\eta \to \infty$. If there exist roots of λ for (3.28), these roots will be the asymptotes of the $\lambda_{(i)} - \eta$ curves. We may factor $P_1(\lambda, \beta)$ as given in (3.4) into

$$P_{1}(\lambda, \beta) = \frac{1}{\lambda^{6}} (\lambda - 1)^{4} f_{1}^{2}(\lambda) f_{2}(\lambda, \beta), \qquad (3.29)$$

where

$$f_1(\lambda) = (\lambda^3 - 3\lambda^2 - \lambda - 1), \qquad (3.30)$$

$$f_{2}(\lambda, \beta) = (\beta - 1)^{2} \lambda^{3} - [3(\beta - 1)^{2} + 4\beta] \lambda^{2} - [(\beta - 1)^{2} + 8\beta] \lambda - (\beta - 1)^{2} - 4\beta.$$
(3.31)

The factors $f_1(\lambda)$ and $f_2(\beta,\lambda)$ are exactly the same as those obtained by Kim [13] in his study of the three-ply problem. The equation $f_1(\lambda)=0$ has one real root λ_{∞} given by

$$\lambda_{\infty} = 1 + \sqrt[3]{2 + \sqrt{4 - (4/3)^3}} + \sqrt[3]{2 - \sqrt{4 - (4/3)^3}} = 3.38297577...$$
 (3.32)

With the exception of $\beta=1$, the factor $f_2(\lambda,\beta)=0$ also yields exactly one real root $\lambda_{\infty,\,\beta}$ for all finite $\beta>0$. Denote this second asymptotic root by $\lambda_{\infty,\,\beta}$ to acknowledge its dependence on β . To understand this β dependence, consider the cases $\beta=0,\,\beta\to\infty$ and $\beta=1$. Starting with $\beta=0$, note that $f_2(\lambda,0)=\lambda^3-3\lambda^2-\lambda-1=f_1(\lambda)$. It follows that $\lambda_{\infty,\,\beta=0}=\lambda_{\infty}$ as given in (3.32). For large β ,

$$f_2(\lambda, \beta) - \beta^2(\lambda^3 - 3\lambda^2 - \lambda - 1) + O(\beta)$$
 (3.33)

The dominant item in $f_2(\lambda, \beta)$ gives $\lim_{\beta \to \infty} \lambda_{\infty, \beta} = \lambda_{\infty}$ again as in (3.32). For $\beta=1$, (3.31) gives that

$$f_2(\lambda, 1) = -4(\lambda + 1)^2,$$
 (3.34)

which has no roots in the range of $\lambda>0$. We have solved the equation $f_2(\lambda,\beta)=0$ numerically and obtained $\lambda_{\infty,\beta}(\beta)$ in Figure 3.3. It is found that

$$\lim_{\beta \to 1} \lambda_{\infty, \beta}(\beta) = \infty, \tag{3.35}$$

and

$$\lambda_{\infty, \beta} > \lambda_{\infty}$$
, for $0 < \beta < \infty$. (3.36)

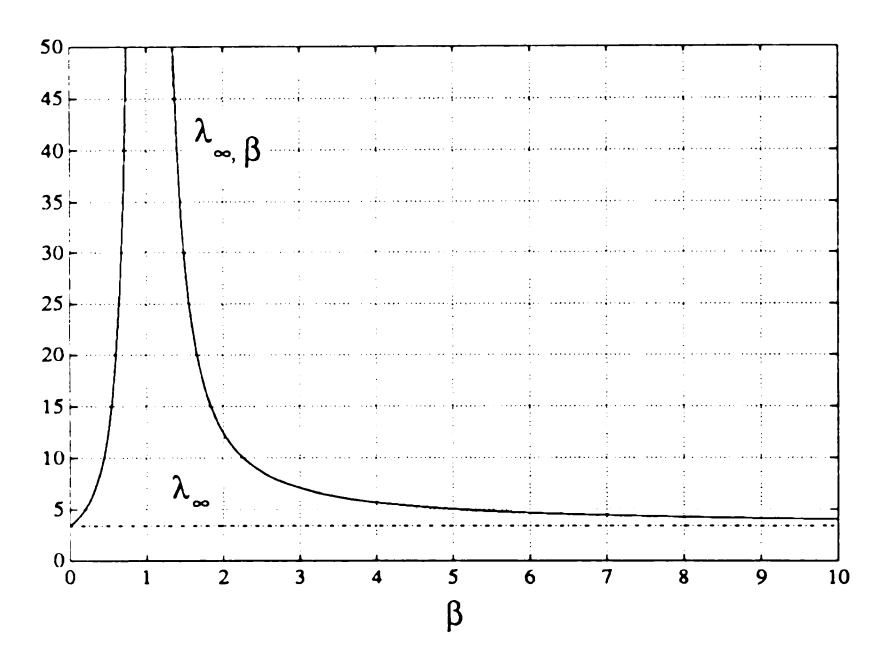


Figure 3.3. The picture of λ_{∞} , $\lambda_{\infty,\beta}(\beta)$.

The values λ_{∞} and $\lambda_{\infty, \beta}$ give all possibilities for roots λ to (2.67) as $\eta \to \infty$ and hence each of the 3 functions $\Phi_i(\eta, \beta, \alpha)$ must approach one of the two of these values as $\eta \to \infty$. Numerically we find that

$$\lim_{\eta \to \infty} \Phi_{1}(\eta, \beta, \alpha) = \lambda_{\infty},$$

$$\lim_{\eta \to \infty} \Phi_{2}(\eta, \beta, \alpha) = \lambda_{\infty},$$

$$\lim_{\eta \to \infty} \Phi_{3}(\eta, \beta, \alpha) = \lambda_{\infty, \beta}.$$

$$(3.37)$$

Note from (3.36), $(3.25)_2$ and $(3.37)_2$ that

$$\Phi_2(\eta, \beta, \alpha) - \lambda_{\infty, \beta} = 0 \tag{3.38}$$

must have at least one root. By evaluating $\Psi(\lambda_{\infty}, \eta, \beta, \alpha)$ with changing η and fixed Pairs of (β, α) , we find that

$$\Psi\left(\lambda_{\infty}, \eta, \beta, \alpha\right) > 0. \tag{3.39}$$

Furthermore by evaluating $\Psi(\lambda_{\infty,\beta},\eta,\beta,\alpha)$ with changing η and fixed pairs of (β,α)

we find that there is exactly one value of $\eta = \eta_{\lambda}$ such that

$$\Psi(\lambda_{\infty,\beta}(\beta), \eta, \beta, \alpha) > 0, \quad \text{if } \eta < \eta_{\lambda};
\Psi(\lambda_{\infty,\beta}(\beta), \eta, \beta, \alpha) < 0, \quad \text{if } \eta > \eta_{\lambda}.$$
(3.40)

So η_{λ} , satisfying

$$\Phi_2(\eta_{\lambda}, \beta, \alpha) - \lambda_{\infty, \beta} = 0. \tag{3.41}$$

is the unique root of equation (3.38). This, in conjunction with (3.36), $(3.25)_2$, $(3.37)_2$ and (3.39), gives

$$\Phi_{1}(\eta, \beta, \alpha) < \lambda_{\infty} < \Phi_{2}(\eta, \beta, \alpha) \quad \text{and} \quad \lambda_{\infty, \beta} < \Phi_{3}(\eta, \beta, \alpha).$$
(3.42)

3.3. Numerical Analysis

A numerical procedure is developed to solve $\Psi(\lambda,\eta,\beta,\alpha)=0$ for each of the three roots $\lambda=\Phi_i(\eta,\beta,\alpha)$ (i=1,2,3) at each fixed material parameters (β,α) and each fixed mode parameter η . The bisection method [11] is employed to do this. It requires to separate these roots from each other in advance of employing the bisection method. For example to determine the first root $\Phi_1(\eta,\beta,\alpha)$, bisection can proceed starting with bounds of 1 and λ_∞ according to (3.23), (3.42). The major difficulty stems from separating the second and third roots, since for small value of η , both roots are bounded below by λ_∞, β . In this case it is necessary to obtain a "separation value" λ_∞ that is simultaneously an upper bound for $\Phi_2(\eta,\beta,\alpha)$ and a lower bound for $\Phi_3(\eta,\beta,\alpha)$ before beginning the bisection process. One such separation value is given by a stationary value (guaranteed to exist by Rolle's theorem) which solves

$$\frac{\partial}{\partial \lambda} \Psi (\lambda, \eta, \beta, \alpha) = 0. \tag{3.43}$$

A numerical procedure has been developed employing a quadratic approximation method [12] for finding λ_{tep} . This method, at given material parameters (β,α) and given mode parameter η , use a quadratic function iteratively to approximate $\Psi(\lambda,\eta,\beta,\alpha)$ and finally to get the local stationary value. Once such a separation value

is obtained, bisection for the second root proceeds by using bounds λ_{∞} and λ_{sep} , and bisection for the third root proceeds by using λ_{sep} and a sufficiently large number. A graphic interpretation of this procedure is shown in Figure 3.4.

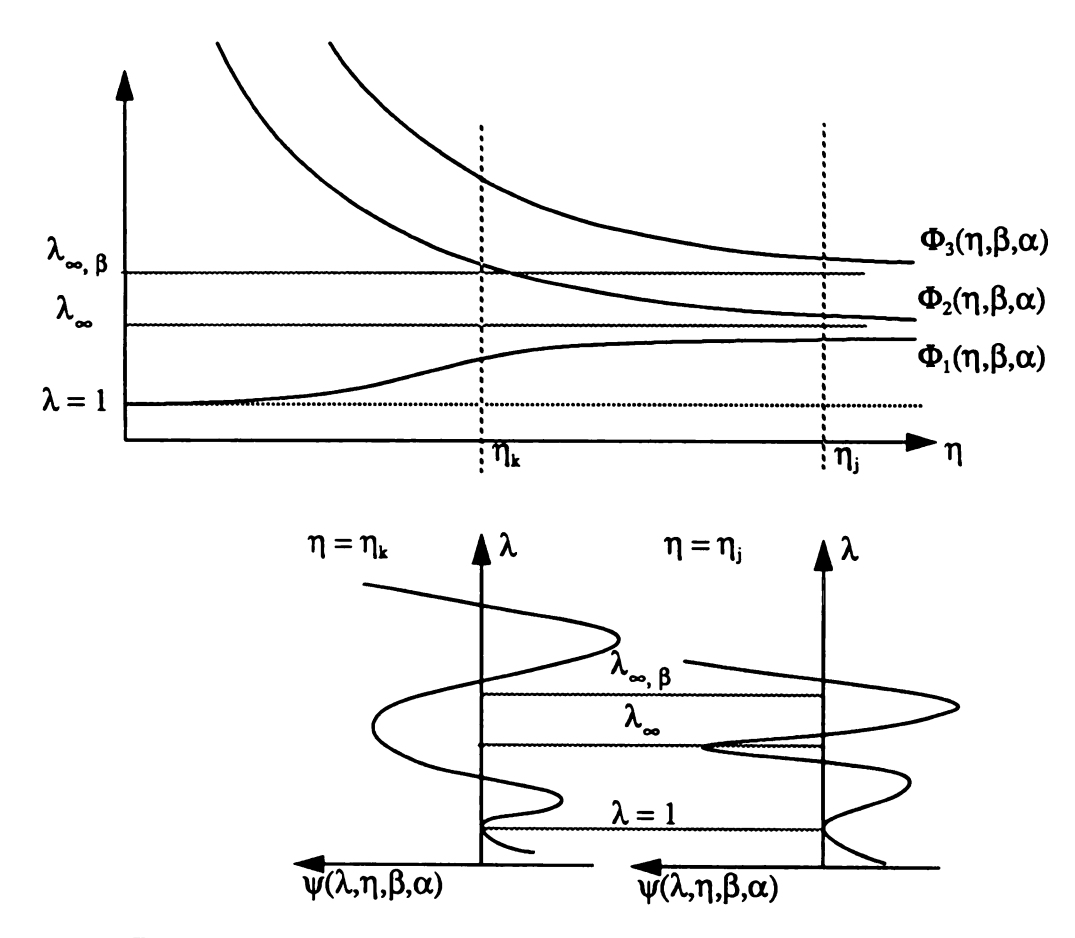


Figure 3.4. A graphic interpretation of the numerical procedure used to obtain $\lambda=\Psi_i(\eta,\beta,\alpha)$ (i=1,2,3).

For the purpose of obtaining complete $\lambda-\eta$ curves $\lambda=\Phi_i(\eta,\beta,\alpha)$ (i=1,2,3) at given pairs of (β,α) , we set up a series of $\{\eta_i\}_{i=1}^n$ such that

$$0 < \eta_1 < \eta_2 < \dots < \eta_n, \tag{3.44}$$

where η_n is the upper bound of the range of η to be considered. We then use the approach discussed above to obtain

$$\lambda_{ik} = \Phi_i(\eta_k, \beta, \alpha) \qquad i = 1, 2, 3 \tag{3.45}$$

obeying

$$\Psi(\lambda_{ik}, \eta_k, \beta, \alpha) = 0, \qquad (3.46)$$

k=1,2,...,n. Thus we can get a series $\{(\lambda_{ik},\eta_k)\}_{k=1}^n$ (i=1,2,3) of which the interpolations are our curve presentations of $\lambda = \Phi_i(\eta,\beta,\alpha)$ (i=1,2,3). If n is large enough, then these interpolations are a good approximation of $\lambda = \Phi_i(\eta,\beta,\alpha)$ (i=1,2,3).

Actually, in our numerical procedure η changes its value backwards, i.e., η changes its value in the order of η_n , η_{n-1} , ..., η_1 . In implementing the numerical procedure, we use the quadratic approximation method to obtain λ_{rep} for the first two values of η (i.e. η_n and η_{n-1}). For the sake of saving computer time, we have found that the following algorithm is able to give a separation point for all subsequent values of η (i.e. η_{n-2} , η_{n-3} , ..., η_1). Namely we use linear extrapolation to approximate the second and third roots $\lambda_{ik} = \Phi_i(\eta_k, \beta, \alpha)$, k=n-2, n-3, ..., 1 and i=2, 3, as

$$\tilde{\lambda}_{ik} = \frac{\lambda_{ik+1} - \lambda_{ik+2}}{\eta_{k+1} - \eta_{k+2}} (\eta_k - \eta_{k+1}) \qquad k = n-2, n-3, ..., 1 \qquad i = 2, 3. \quad (3.47)$$

Then the separation value λ_{sep} is given by

$$\lambda_{sep} = \frac{\tilde{\lambda}_{2k} + \tilde{\lambda}_{3k}}{2}$$
 $k = n - 2, n - 3, ..., 1.$ (3.48)

Figure 3.5-3.11 are examples of the curve presentations of $\lambda = \Phi_i(\eta, \beta, \alpha)$ (i=1,2,3) carried out for pairs of (β, α) specified beneath each picture. The set of pairs of (β, α) calculated is the Cartesian product of $\alpha \in \{0.0, 0.1, 0.2, ..., 1.0\}$ and $\beta \in \{1, 2, 3, ..., 10\}$. Among these cases with $\beta = 1$ or $\alpha = 0$ or 1 reduce to that of a noncomposite material construction and curves of these cases are precisely the same as those obtained by Sawyers and Rivlin [3] [4]. The third root $\Phi_3(\eta, \beta, \alpha)$ moves up to infinity as $\beta \to 1$, $\alpha \to 0$, or $\alpha \to 1$ as can be seen in these figures. For each pair of (β, α) the first root $\Phi_1(\eta, \beta, \alpha)$ goes from 1 when $\eta \to 0$ to λ_∞ when $\eta \to \infty$, the second root $\Phi_2(\eta, \beta, \alpha)$ goes from infinity when $\eta \to 0$ to λ_∞ when $\eta \to \infty$, and the third

root $\Phi_3(\eta,\beta,\alpha)$ goes from infinity when $\eta\to 0$ to $\lambda_{\infty,\,\beta}$ when $\eta\to\infty$. For some pairs of (β,α) , the functions $\Phi_1(\eta,\beta,\alpha)$ and $\Phi_2(\eta,\beta,\alpha)$ are not monotone as shown in Figure 3.10 and 3.11.

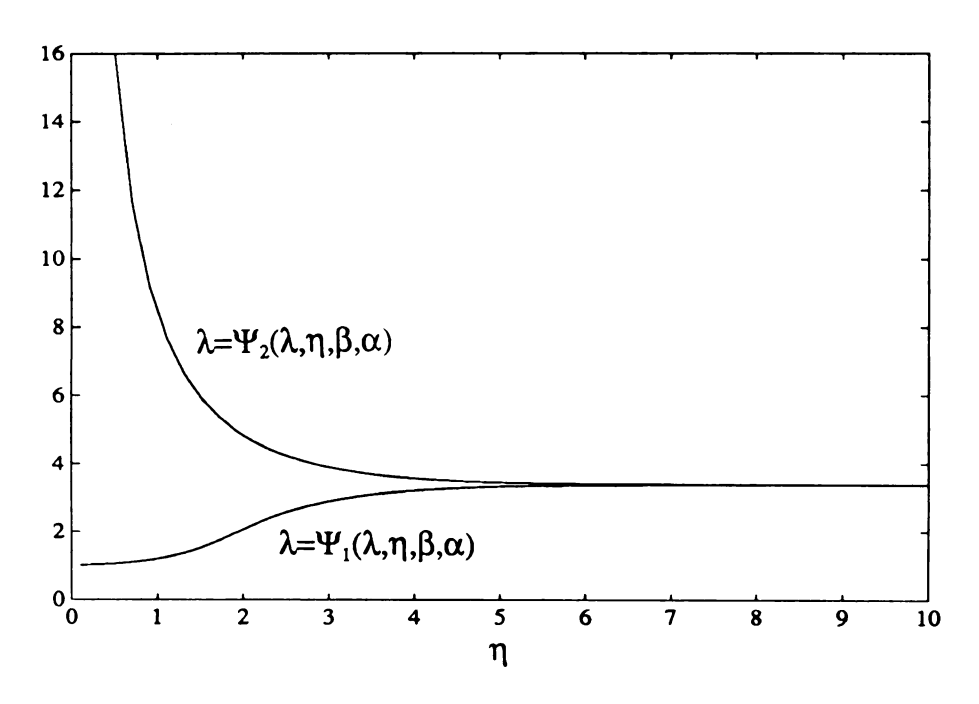


Figure 3.5. The λ vs. η curves $\lambda_i = \Phi_i(\eta, \beta, \alpha)$ at $\beta = 1$, $\alpha = 0.3$.

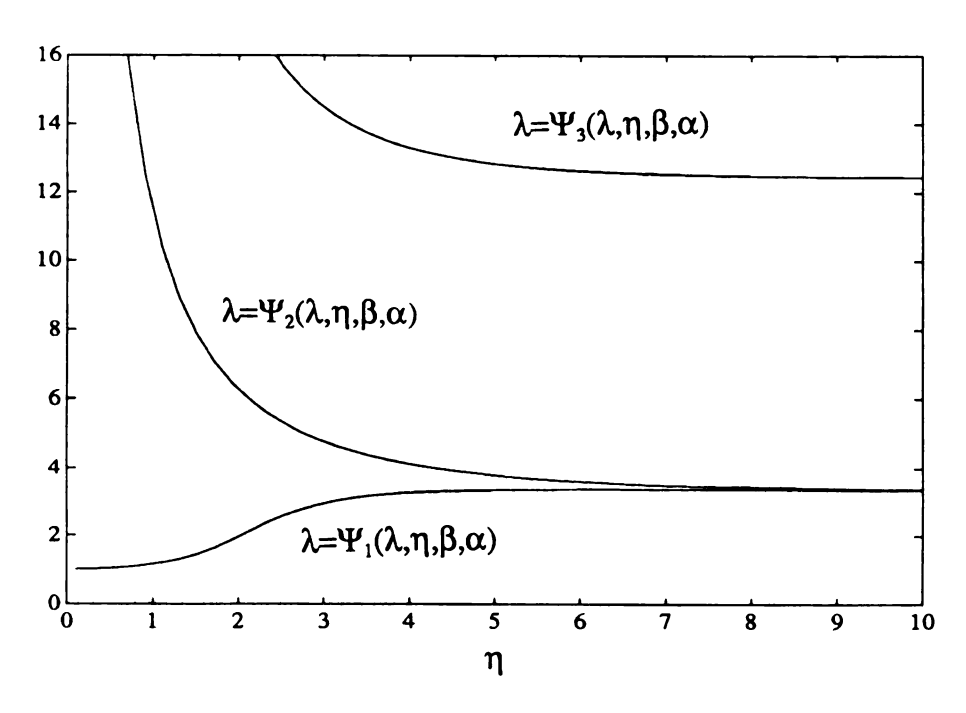


Figure 3.6. The λ vs. η curves $\lambda_i = \Phi_i(\eta, \beta, \alpha)$ at $\beta = 2$, $\alpha = 0.3$.

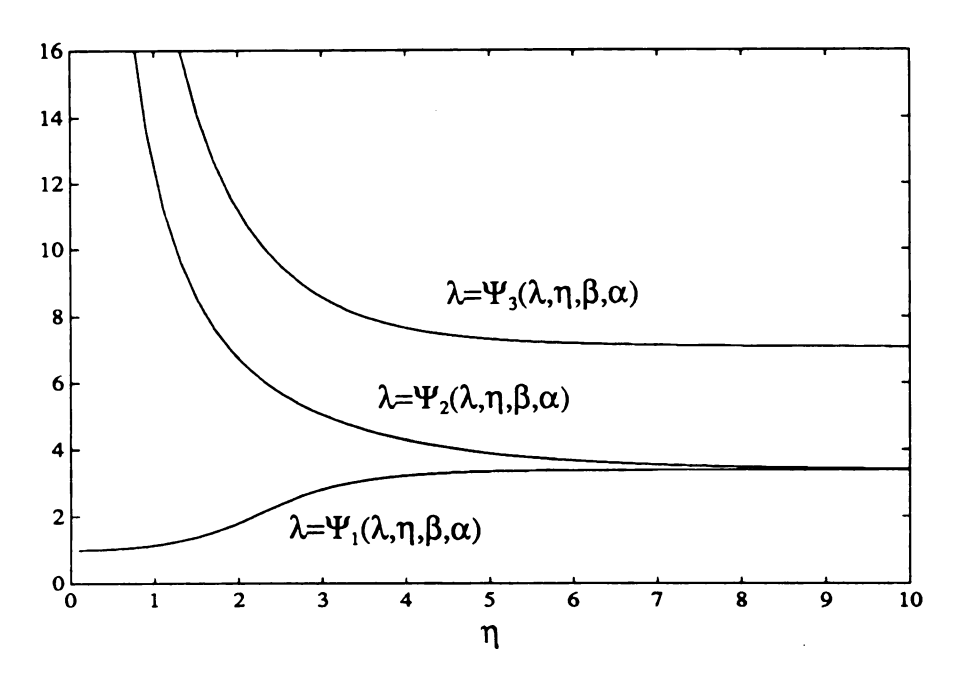


Figure 3.7 The λ vs. η curves $\lambda_i {=} \Phi_i(\eta,\beta,\alpha)$ at $\beta {=} 3,~\alpha {=} 0.3.$

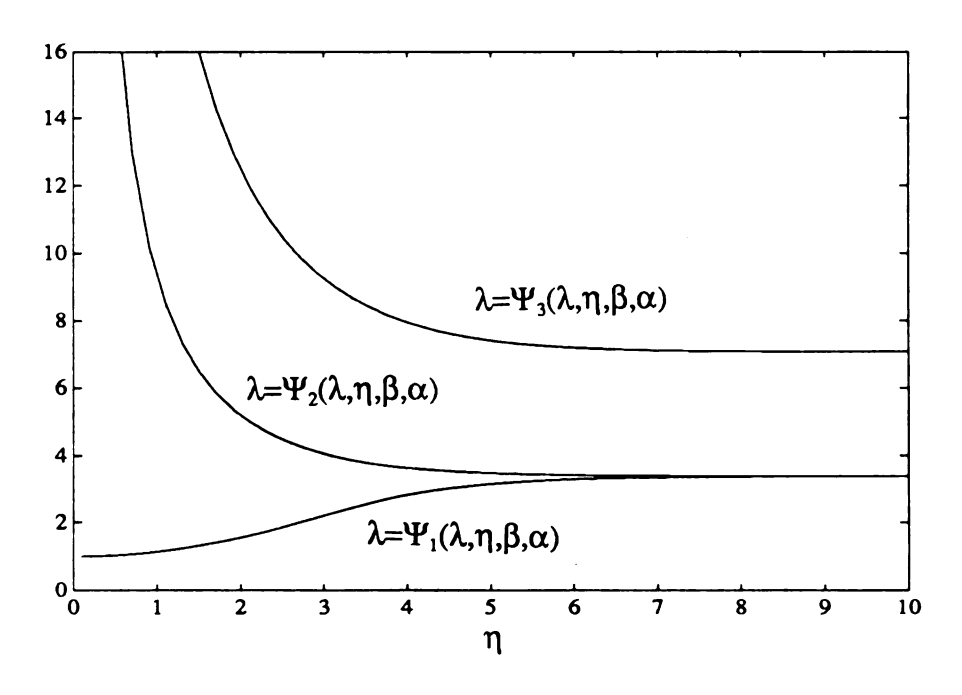


Figure 3.8. The λ vs. η curves $\lambda_i = \Phi_i(\eta, \beta, \alpha)$ at $\beta = 3$, $\alpha = 0.5$.

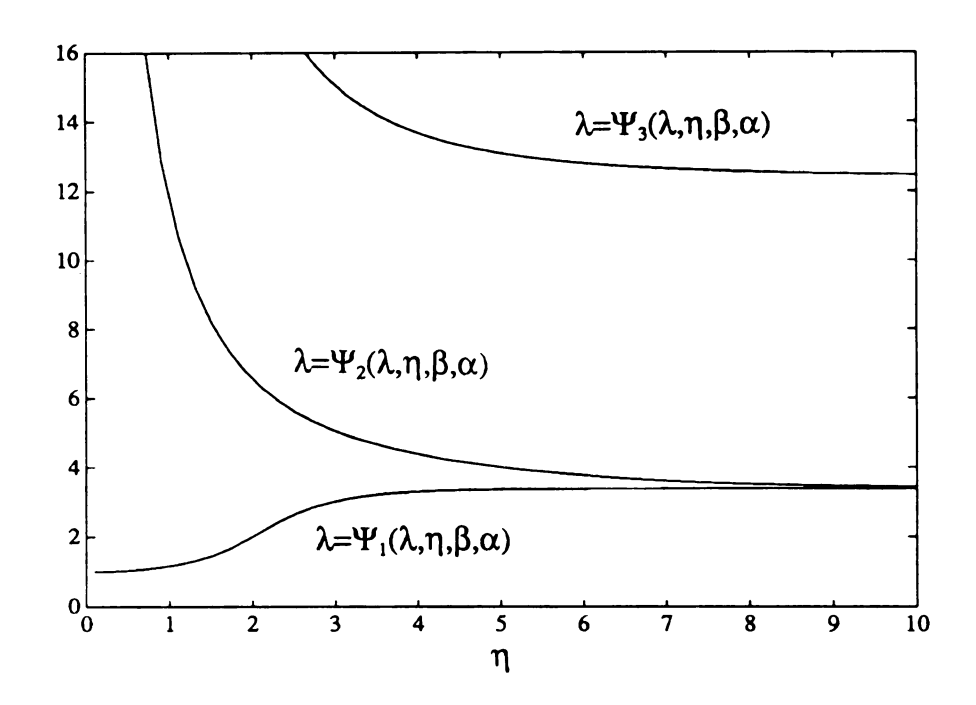


Figure 3.9. The λ vs. η curves $\lambda_i = \! \Phi_i(\eta,\beta,\alpha)$ at $\beta = \! 2,~\alpha = \! 0.25.$

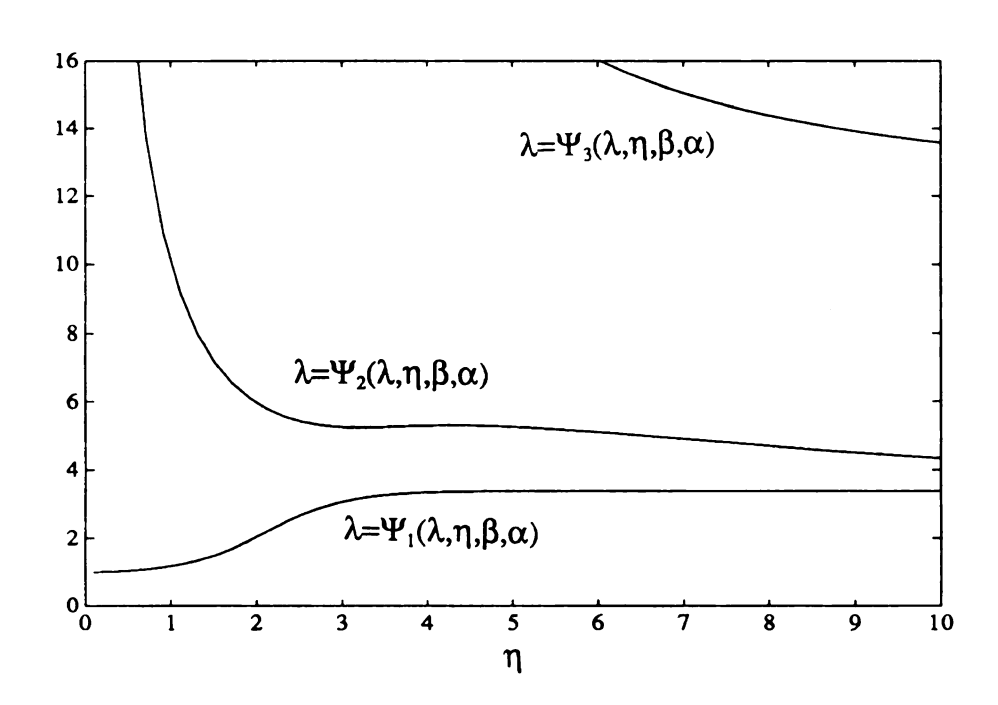


Figure 3.10. The λ vs. η curves $\lambda_i = \Phi_i(\eta, \beta, \alpha)$ at $\beta = 2$, $\alpha = 0.1$.

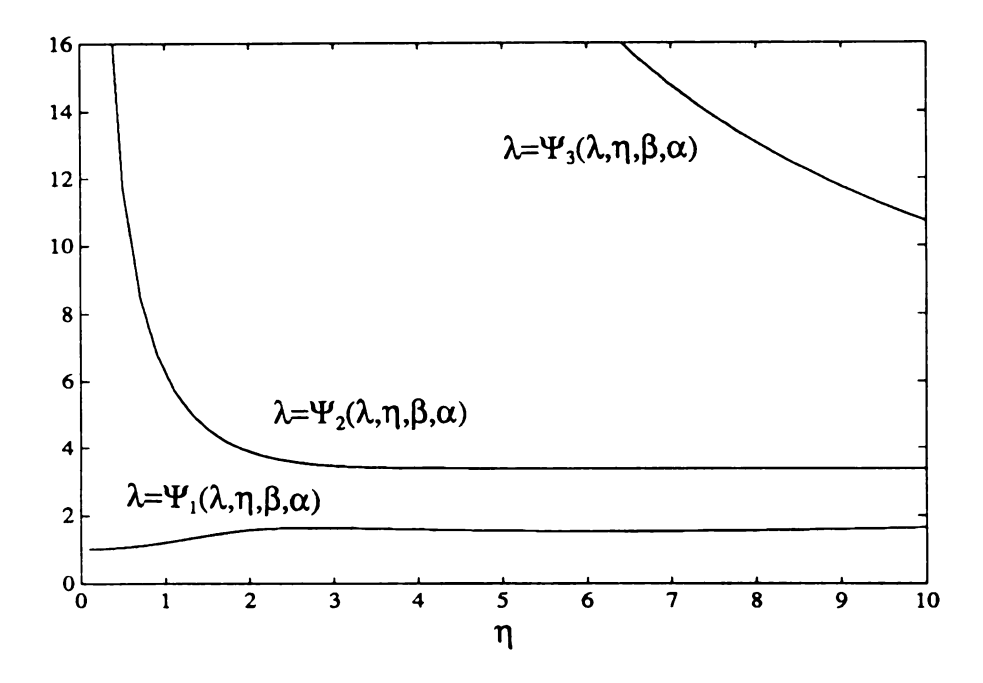


Figure 3.11. The λ vs. η curves $\lambda_i = \Phi_i(\eta, \beta, \alpha)$ at $\beta = 4$, $\alpha = 0.9$.

In chapter 2 we have formulated the equations for the problem of the buckling instability of the two-ply composite plate. A set of computer program has been coded for solving these equations according to the discussion in chapter 3 and 4. With these computer program we can predict the failure stretch ratio λ and then, following (2.51), the failure thrust T for given material construction ((β , α), l_1 , l_2 , l_3). Note from (2.51) that the failure thrust T is monotone increasing with λ . Denote T_m^i for failure thrust at mode number m and corresponding to $\lambda = \Phi_i(\eta_m = m\pi l_2/l_1, \beta, \alpha)$ (i=1,2,3). It follows from (3.23) and (3.42) that

$$T_{m}^{1} < T_{\infty} < T_{m}^{2} < T_{m}^{3}. \tag{3.49}$$

This gives that the critical failure thrust always corresponds to $\lambda = \Phi_1(\eta, \beta, \alpha)$.

As Sawyers and Rivlin [3] [4] as well as Pence and Song [9] [10] have pointed out, the failure thrusts for noncomposite material construction are ordered as

$$0 < T_1^1 < T_2^1 < \dots < T_{\infty}^2 < \dots < T_2^2 < T_1^2. \tag{3.50}$$

This is the direct deduction from the fact that for noncomposite material construction,

 $\lambda = \Phi_1(\eta, \beta, \alpha)$ is always monotonically increase with η and $\lambda = \Phi_2(\eta, \beta, \alpha)$ is always monotonically decrease with η . In the case of composite material construction, as can been seen in figure 3.10 and figure 3.11, some pairs of (β, α) no longer gives $\Phi_1(\eta, \beta, \alpha)$ monotonically increasing in η and some no longer gives $\Phi_2(\eta, \beta, \alpha)$ monotonically decreasing in η . These cause a reordering of failure thrusts, i.e., for some m<n

$$T_n^1 < T_m^1$$
 and $T_m^2 < T_n^2$. (3.51)

4. **DEFORMATION**

The deformation of a thick rectangular nonlinear elastic composite plate consisting of two plies of different shear moduli under thrust has been treated as a homogefinite deformation superposed with an incremental nonhomogeneous neous deformation. The incremental deformations are allowed to take place if and only if there exists a nontrivial solution for equation (2.60). For a specified material construction, the material parameter pair (β,α) and plate aspect ratio 1/1 are given. For a given number of half wavelengths m, then the parameter η is determined. There are 3 thrusts T which support bifurcation of solutions for each such half wavelength possibility m. They are determined by the 3 load parameters $\lambda = \Phi_i(\eta, \beta, \alpha)$ (i=1,2,3). We now examine the deformation corresponding to these 3 different possibilities. By substituting $\lambda = \Phi_i(\eta,\beta,\alpha$) (i=1,2 or 3) into (2.60) and solving it, we can obtain a nontrivial solution vector 1. Then $U_2(X_2)$ and $U_1(X_2)$ can be obtained from (2.55) and (2.49)₃. Furthermore u_1 and u_2 are obtained according to (2.47) or (2.48). We rewrite $U_2(X_2)$ and I here for the convenience of discussion:

$$U_{2}^{(j)} = L_{1}^{(j)} \cosh(\Omega X_{2}) + L_{2}^{(j)} \sinh(\Omega X_{2}) + M_{1}^{(j)} \cosh(\lambda \Omega X_{2}) + M_{2}^{(j)} \sinh(\lambda \Omega X_{2}),$$

$$(4.1)$$

where j = 1, 2 for ply-1 or ply-2. The solution vector

$$I = \{L_1^{(1)}, L_2^{(1)}, M_1^{(1)}, M_2^{(1)}, L_1^{(2)}, L_2^{(2)}, M_1^{(2)}, M_2^{(2)}\}^T,$$
(4.2)

is normalized so that

$$\|\mathbf{l}\|_{2}^{2} = \mathbf{l}^{T}\mathbf{l} = 1. \tag{4.3}$$

Thus the full deformation \hat{x} can be obtained. Figure 4.1 - Figure 4.3 are three examples of the full deformation corresponding to $\Phi_1(\eta,\beta,\alpha)$, $\Phi_2(\eta,\beta,\alpha)$ and $\Phi_3(\eta,\beta,\alpha)$ respectively for a case of m=2, l_1 =1.2, l_2 =1.0. In these figures, ϵ is chosen to make the deformed configurations distinguishable. (In Figure 4.1-4.3, dot line: original configuration, dash line: homogeneous deformation, solid line: buckled deformation).

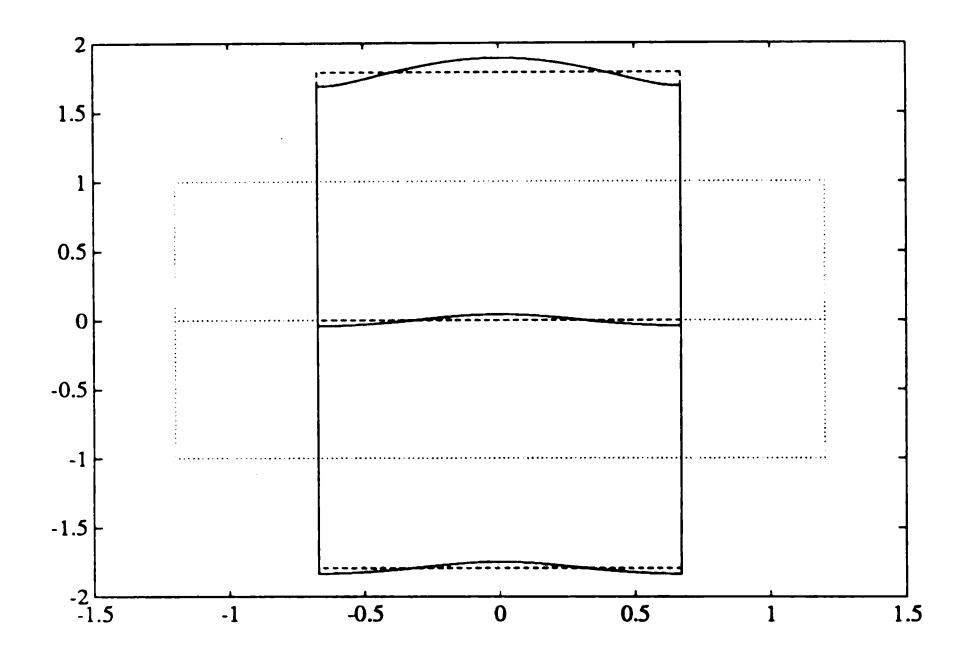


Figure 4.1. Deformation of the 2-ply composite plate under thrust where ϵ =0.1, m=2, so that η =m π l₂/l₁=5.236, β =3, α =0.5 and λ = Φ ₁(5.236,3,0.5)=3.199.

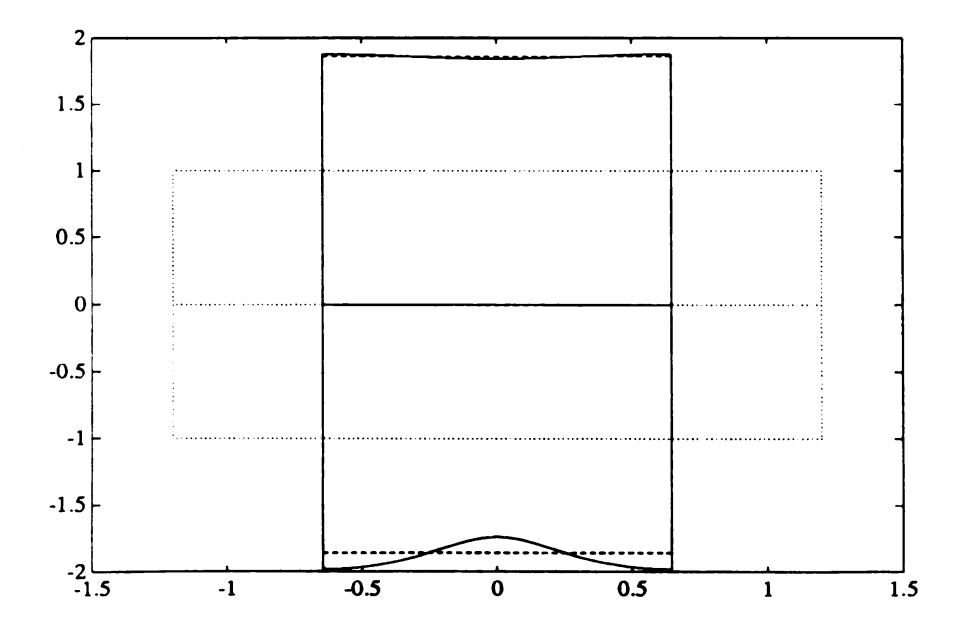


Figure 4.2 Deformation of the 2-ply composite plate under thrust where ϵ =0.05, m=2, so that η =m π l₂/l₁=5.236, β =3, α =0.5 and λ = Φ ₂(5.236,3,0.5)=3.457.

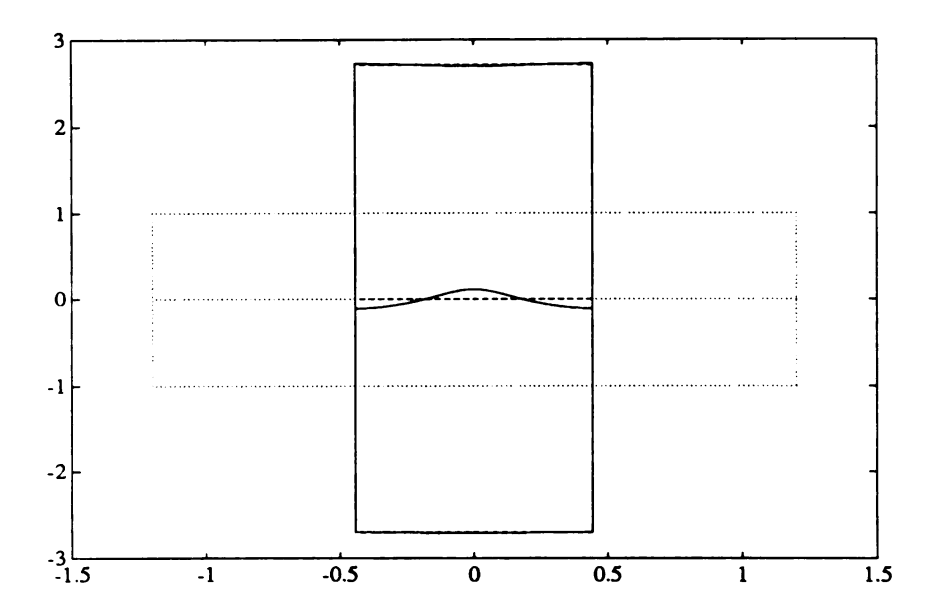


Figure 4.3 Deformation of the 2-ply composite plate under thrust where ϵ =0.3, m=2, so that η =m π l₂/l₁=5.236, β =3, α =0.5 and λ = Φ ₃(5.236,3,0.5)=7.345.

Sawyers and Rivlin [3] [4] have shown that all buckled plane deformations of the type under consideration may be classified as either flexure or barrelling for non-composite cases. A flexural deformation is defined to be one for which U_2 is an even function with respect to X_2 , and a barrelling deformation is defined to be one for which U_2 is an odd function with respect to X_2 . Pence and Song have also shown that flexural and barrelling deformations take place in the symmetric three-ply problem [10]. In the three-ply problem studied in [10], the composite plate considered is symmetric in the X_2 direction. One can then split the (12×12) linear system of the three-ply problem (similar to (2.60) here) into two separate (6×6) subsystems by making use of the symmetry. One subsystem then gives the flexure deformations and the other gives barrelling deformations.

In the two-ply problem studied here, recall from (2.64) that if $\beta=1$, $\alpha=0$ or $\alpha=1$, then the problem reduces to a noncomposite one. In these cases we have obtained the same result as found by Sawyers and Rivlin [3] [4]. As mentioned in Section 3.1,

there are two roots $\Phi_1(\eta,\beta,\alpha)$ and $\Phi_2(\eta,\beta,\alpha)$ (given by (3.24)) for equation (2.67) for noncomposite cases. The solution vector I corresponding to $\Phi_1(\eta,\beta,\alpha)$ and $\Phi_2(\eta,\beta,\alpha)$ then gives a pure flexural deformation and a pure barrelling deformation respectively.

In general, if the material construction of the two-ply plate is truly composite $(\beta \neq 1, \alpha \neq 0 \text{ and } \alpha \neq 1)$, then the symmetry with respect to X_2 no longer exists. The solution vector \mathbf{I} obtained as mentioned above makes U_2 , as given by (4.1), neither an even function of X_2 nor an odd function of X_2 . Neither of the $\Phi_i(\eta, \beta, \alpha)$ (i=1,2,3) will then correspond to pure flexure or pure barrelling. In the two-ply problem, buckling deformations $\hat{\mathbf{x}}$ as given by(2.33) associated with $\Phi_1(\eta, \beta, \alpha)$, $\Phi_2(\eta, \beta, \alpha)$ and $\Phi_3(\eta, \beta, \alpha)$ have a mixed mode flexure and barreling character.

In order to examine the characters combining the mixed-mode, we decompose the vector I by

$$\mathbf{l} = \mathbf{a} + \mathbf{b} + \mathbf{c} + \mathbf{d}, \tag{4.4}$$

$$\mathbf{a} = \{a_1, 0, a_3, 0, a_5, 0, a_7, 0\}^T, \tag{4.5}$$

$$\mathbf{b} = \{0, b_2, 0, b_4, 0, b_6, 0, b_8\}^T, \tag{4.6}$$

$$\mathbf{c} = \{0, c_2, 0, c_4, 0, c_6, 0, c_8\}^T, \tag{4.7}$$

$$\mathbf{d} = \{d_1, 0, d_3, 0, d_5, 0, d_7, 0\}^T, \tag{4.8}$$

where

$$a_{1} = a_{5} = \frac{L_{1}^{(1)} + L_{1}^{(2)}}{2}, \qquad a_{3} = a_{7} = \frac{M_{1}^{(1)} + M_{1}^{(2)}}{2},$$

$$b_{2} = b_{6} = \frac{L_{2}^{(1)} + L_{2}^{(2)}}{2}, \qquad b_{4} = b_{8} = \frac{M_{2}^{(1)} + M_{2}^{(2)}}{2},$$

$$c_{2} = -c_{6} = \frac{L_{2}^{(1)} - L_{2}^{(2)}}{2}, \qquad c_{4} = -c_{8} = \frac{M_{2}^{(1)} - M_{2}^{(2)}}{2},$$

$$d_{1} = -d_{5} = \frac{L_{1}^{(1)} - L_{1}^{(2)}}{2}, \qquad d_{3} = -d_{7} = \frac{M_{1}^{(1)} - M_{1}^{(2)}}{2}.$$

$$(4.9)$$

This decomposition, in the sense of 2-norm, satisfies

$$\|\mathbf{l}\|_{2}^{2} = \|\mathbf{a}\|_{2}^{2} + \|\mathbf{b}\|_{2}^{2} + \|\mathbf{c}\|_{2}^{2} + \|\mathbf{d}\|_{2}^{2}. \tag{4.10}$$

By this decomposition, the solution for the ordinary differential equation (2.52), U_2 , is expressed as

$$U_2 = U_2^a + U_2^b + U_2^c + U_2^d (4.11)$$

where

$$U_2^a = a_1 \cosh(\Omega X_2) + a_3 \cosh(\lambda \Omega X_2), \quad -R_1 \le X_2 \le R_2,$$
 (4.12)

$$U_2^b = b_2 sinh(\Omega X_2) + b_4 sinh(\lambda \Omega X_2), \quad -R_1 \le X_2 \le R_2,$$
 (4.13)

$$U_{2}^{c} = \begin{cases} c_{2} \sinh \left(\Omega X_{2}\right) + c_{4} \sinh \left(\lambda \Omega X_{2}\right), & -R_{1} \leq X_{2} \leq 0, \\ -c_{2} \sinh \left(\Omega X_{2}\right) - c_{4} \sinh \left(\lambda \Omega X_{2}\right), & 0 \leq X_{2} \leq R_{2}, \end{cases}$$

$$(4.14)$$

$$U_{2}^{d} = \begin{cases} d_{1} cosh (\Omega X_{2}) + d_{3} cosh (\lambda \Omega X_{2}), & -R_{1} \leq X_{2} \leq 0, \\ -d_{1} cosh (\Omega X_{2}) - d_{3} cosh (\lambda \Omega X_{2}), & 0 \leq X_{2} \leq R_{2} \end{cases}$$
(4.15)

Note that the 4 functions in the decomposition have the following symmetry properties

$$U_{2}^{a}(X_{2}) = U_{2}^{a}(-X_{2}), U_{2}^{c}(X_{2}) = U_{2}^{c}(-X_{2}),$$

$$U_{2}^{b}(X_{2}) = -U_{2}^{b}(-X_{2}), U_{2}^{d}(X_{2}) = -U_{2}^{d}(-X_{2}).$$

$$(4.16)$$

We shall say that if **b=0** and **d=0**, then the whole deformation is one of pure flexure, similarly, if **a=0** and **c=0**, then the whole deformation is one of pure barrelling. We now turn to examine the continuity of U_2^a , U_2^c , U_2^b , U_2^d and their derivatives across the interface $X_2=0$. For this purpose it is convenient to introduce the notation $[[]]|_0$ to indicate the jump in value across this interface. Clearly from (4.12), (4.13) it follows that

$$\left[\left[\left(U_{2}^{a}\right)^{(n)}\right]\right]\Big|_{0} = 0, \qquad \left[\left[\left(U_{2}^{b}\right)^{(n)}\right]\right]\Big|_{0} = 0, \tag{4.17}$$

for n=0,1,2,3,... Here (n) denotes derivatives of order n and (0) indicates the undifferentiated function. On the other hand,

$$\left[\left[\left(U_{2}^{c}\right)^{(2n)}\right]\right]\Big|_{0}=0, \qquad \left[\left[\left(U_{2}^{d}\right)^{(2n+1)}\right]\right]\Big|_{0}=0, \tag{4.18}$$

for n=0,1,2,3,.... To address the possible discontinuity in $(U_2^c)^{(2n+1)}$ and $(U_2^d)^{(2n)}$ at the interface $X_2=0$, we note that the interface conditions (2.58)

$$[[U_2]]|_0 = 0, \qquad [[U_2']]|_0 = 0$$
 (4.19)

along with (4.17), (4.18) give

$$\left[\left[(U_2^c)^{(1)} \right] \right]_0 = 0, \qquad \left[\left[(U_2^d)^{(0)} \right] \right]_0 = 0. \tag{4.20}$$

However $(U_2^c)^{(2n+1)}$, $(U_2^d)^{(2n)}$ for n=1,2,3, ... are *not* continuous across the interface $X_2=0$.

Thus by using the boundary and interface conditions, we conclude that in the range of $-R_1 \le X_2 \le R_2$, U_2^a and U_2^b and their derivatives of any order are continuous, $(U_2^c)^{(0)}$, $(U_2^c)^{(1)}$, $(U_2^c)^{(2)}$ and $(U_2^c)^{(2n)}$ are continuous, and $(U_2^d)^{(0)}$, $(U_2^d)^{(1)}$, $(U_2^d)^{(2n+1)}$ are continuous. Furthermore

$$[[U_2^{(2n)}]]\Big|_0 = [[(U_2^d)^{(2n)}]]\Big|_0 = -2(\Omega^{2n}d_1 + (\lambda\Omega)^{2n}d_3), \qquad (4.21)$$

$$[[U_2^{(2n+1)}]]\Big|_0 = [[(U_2^c)^{(2n+1)}]]\Big|_0 = -2(\Omega^{2n+1}c_2 + (\lambda\Omega)^{2n+1}c_4), \quad (4.22)$$

where n = 1, 2, 3,..., and a superscript number n inside parentheses indicates taking the nth derivative, and a superscript number n without parentheses indicates exponentiation to the power of n. According to the above discussion, we may refer to the four parts of deformation relating to U_2^a , U_2^b , U_2^c and U_2^d in the decomposition of U_2 as follows: smooth flexure part, smooth barrelling part, residual flexure part, residual barrelling part respectively. According to (4.15) and $(4.20)_2$

$$d_1 + d_3 = 0. (4.23)$$

Similarly, according to (4.14) and $(4.20)_1$

$$c_2 + \lambda c_4 = 0. \tag{4.24}$$

With equation (4.23) and (4.24), by entering (4.11) into the interface continuity condition (2.13), we find that

$$d_1 = \frac{D_1}{D}a_1 + \frac{D_2}{D}a_3 \tag{4.25}$$

and

$$c_2 = -\frac{D_2}{D}b_2 - \frac{\lambda D_1}{D}b_4, \tag{4.26}$$

where

$$D = (\beta + 1) (1 - \lambda^2), \quad D_1 = (\beta - 1) (1 + \lambda^2), \quad D_2 = 2 (\beta - 1) \lambda^2.$$
 (4.27)

On account of (4.9), (4.16), (4.23)-(4.26), we conclude that if the deformation is one of pure flexure, then $c_2=c_4=c_6=c_8=0$ so that it is in fact smooth flexure. Similarly, if the deformation is one of pure barrelling, then it is in fact smooth barrelling.

5. DISCUSSION

In Chapter 4 we have discussed the decomposition (4.4) of the solution vector from equation (2.60) and the corresponding decomposition (4.11) of the solution to the differential equation (2.52). Since any solution vector of equation (2.60) can be decomposed in this way, it follows that any possible buckling deformation is the combination of flexural and barrelling deformations. Note that this decomposition satisfies (4.10), we further examine how these portions $\|\mathbf{a}\|_{2}^{2}/\|\mathbf{l}\|_{2}^{2}$, $\|\mathbf{b}\|_{2}^{2}/\|\mathbf{l}\|_{2}^{2}$, $\|\mathbf{c}\|_{2}^{2}/\|\mathbf{l}\|_{2}^{2}$ and $\|\mathbf{d}\|_2^2/\|\mathbf{1}\|_2^2$ vary with η . A number of material constructions (β,α) have been computed and these changes have been plotted in curves. Figure 5.2 and 5.3 are included to give an example of these curves. (In Figure 5.2 and 5.3, solid line: $\|\mathbf{a}\|_2^2 / \|\mathbf{l}\|_2^2$, dash line: $\|\mathbf{b}\|_{2}^{2}/\|\mathbf{l}\|_{2}^{2}$, dash-dot line: $\|\mathbf{c}\|_{2}^{2}/\|\mathbf{l}\|_{2}^{2}$, dot line: $\|\mathbf{d}\|_{2}^{2}/\|\mathbf{l}\|_{2}^{2}$). They are the varying portions for $\lambda = \Phi_i(\eta, 3, 0.5)$ (i=1, 2) (see Figure 5.1) respectively. The numerical algorithm used in calculating these curves in Figure 5.3 only gives accurate results for $\eta > 1$, consequently the curves are not shown for $\eta < 1$. In general, in the deformations corresponding to $\Phi_1(\eta,\beta,\alpha)$, smooth flexure dominates the whole deformation; in the deformations corresponding to $\Phi_2(\eta,\beta,\alpha)$, smooth barrelling dominates the whole deformation. Residual flexure and residual barrelling always occupy small portions. Figure 5.4a-5.5d are examples of these decomposed deformations. In these figures, equation (4.3) is again used to establish the over all normalization. (In Figure 5.4a-5.5d, dot line: original configuration, dash line: homogeneous deformation, solid line: buckled deformation portion).

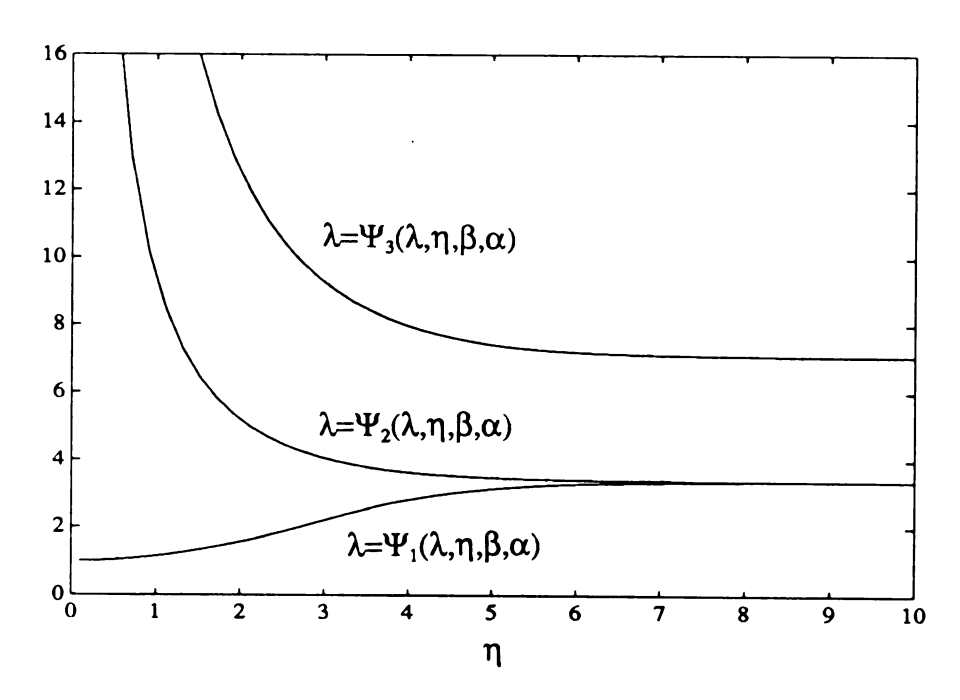


Figure 5.1. The λ vs. η curves $\lambda_i{=}\Phi_i(\eta,\beta,\alpha)$ at $\beta{=}3,~\alpha{=}0.5.$

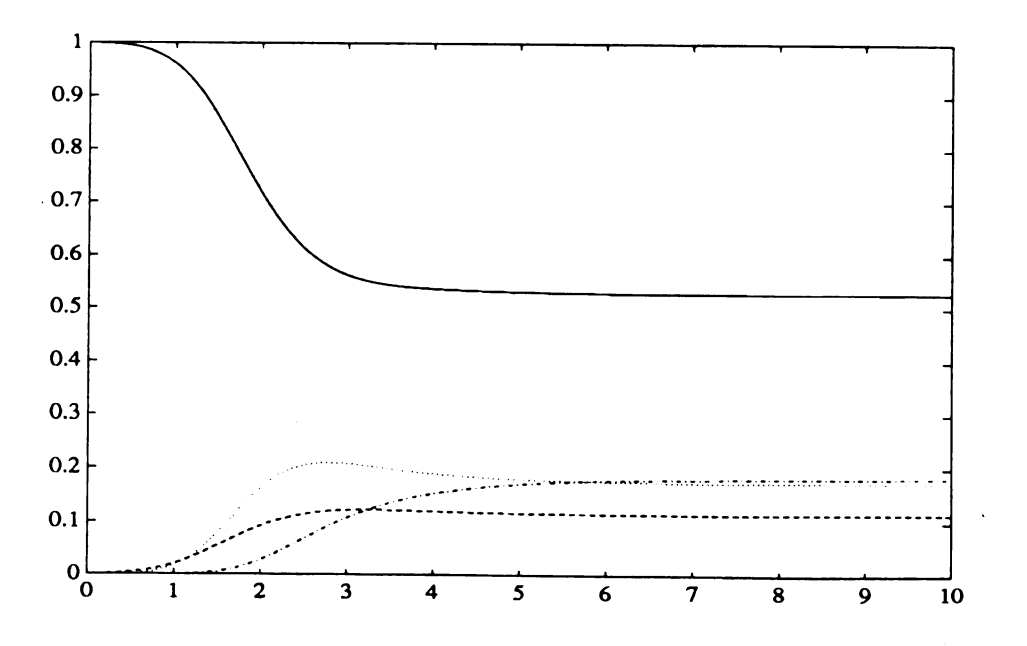


Figure 5.2. An example of the portions of these four type deformations varying with η for the case of β =3, α =0.5, for the first root in λ vs. η curves: λ = $\Phi_1(\eta,3.0,0.5)$.

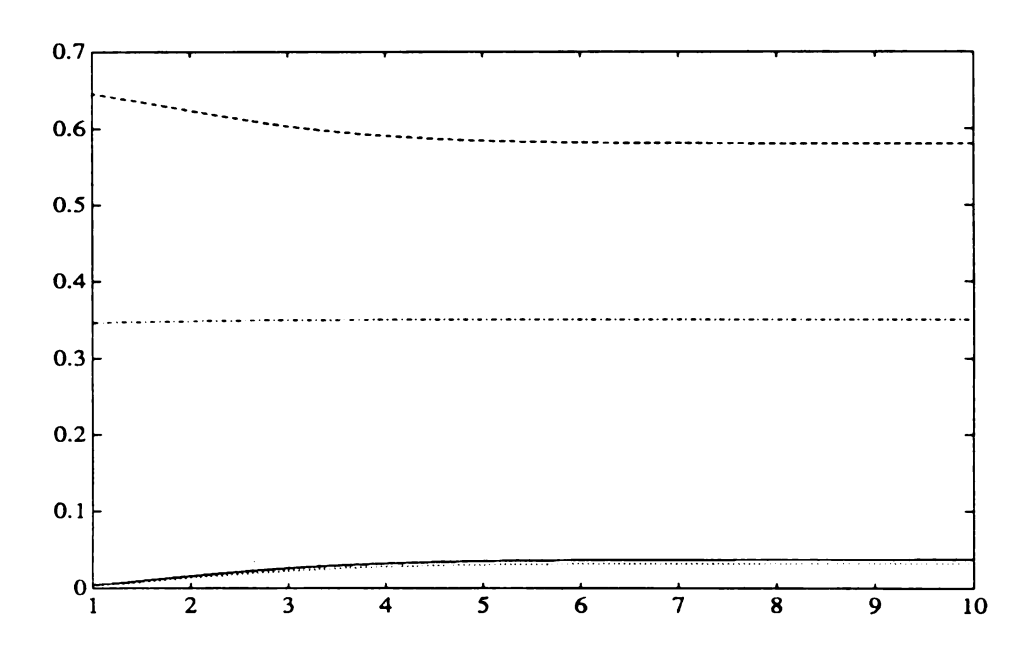


Figure 5.3. An example of the portions of these four type deformations varying with η for the case of β =3, α =0.5, for the second root in λ vs. η curves: λ = $\Phi_2(\eta,3.0,0.5)$.

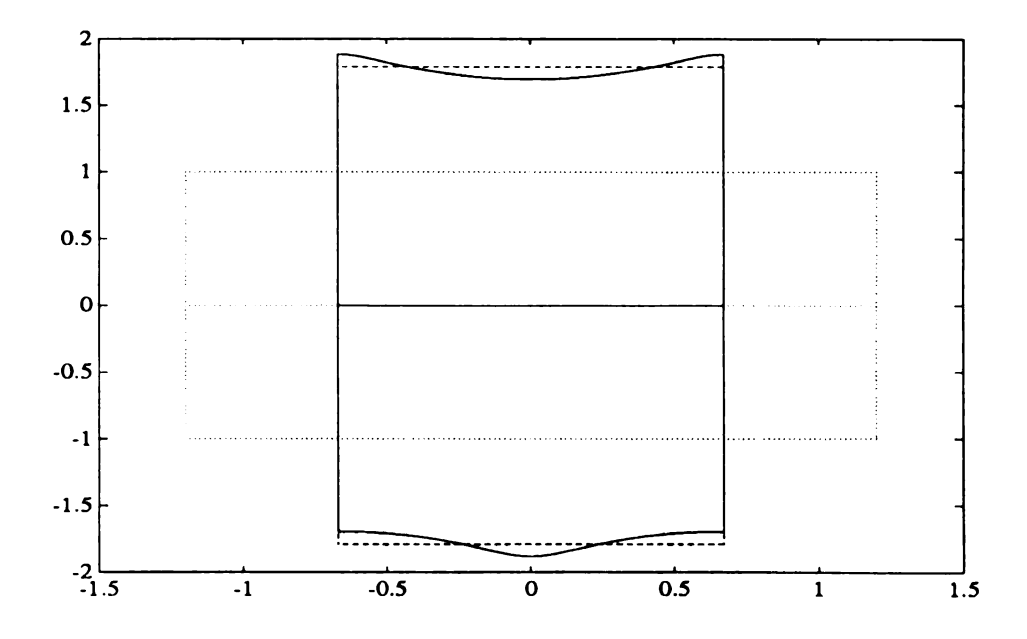


Figure 5.4a. The smooth flexural deformation portion at ϵ =0.0005, m=2, η =5.236, β =3.0, α =0.5, λ = Φ_1 (5.326,3.0,0.5)=3.199. The overall deformation was shown previously in Figure 4.1.

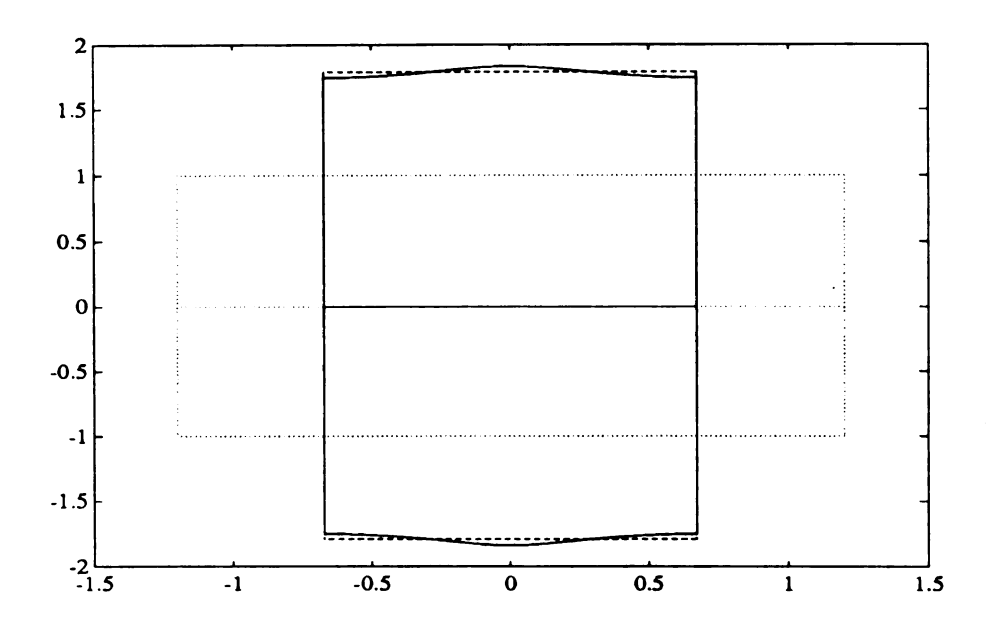


Figure 5.4b. The smooth barrelling deformation portion at ϵ =0.0001, m=2, η =5.236, β =3.0, α =0.5, λ = Φ_1 (5.326,3.0,0.5)=3.199. The overall deformation was shown previously in Figure 4.1.

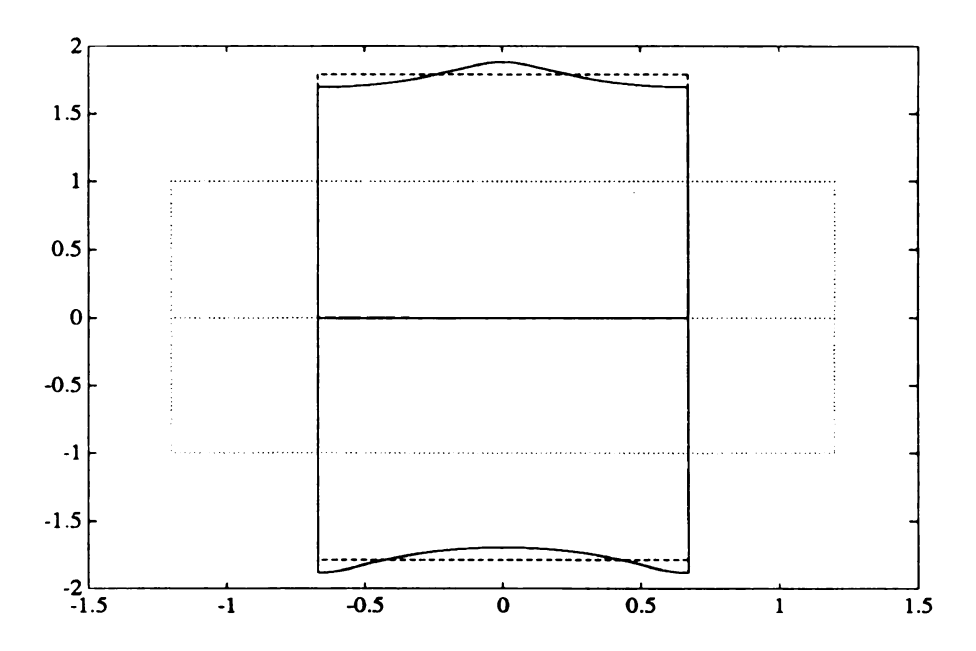


Figure 5.4c. The residual flexural deformation portion at ϵ =0.0001, m=2, η =5.236, β =3.0, α =0.5, λ = Φ_1 (5.236,3.0,0.5)=3.199. The overall deformation was shown previously in Figure 4.1.

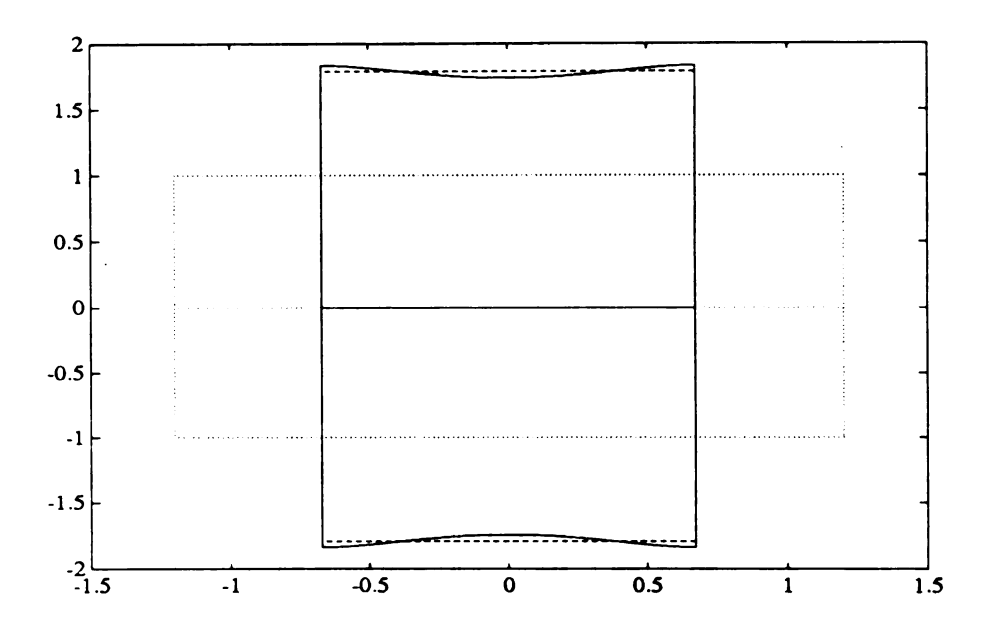


Figure 5.4d. The residual barrelling deformation portion at ϵ =0.0001, m=2, η =5.236, β =3.0, α =0.5, λ = Φ_1 (5.236,3.0,0.5)=3.199. The overall deformation was shown previously in Figure 4.1.

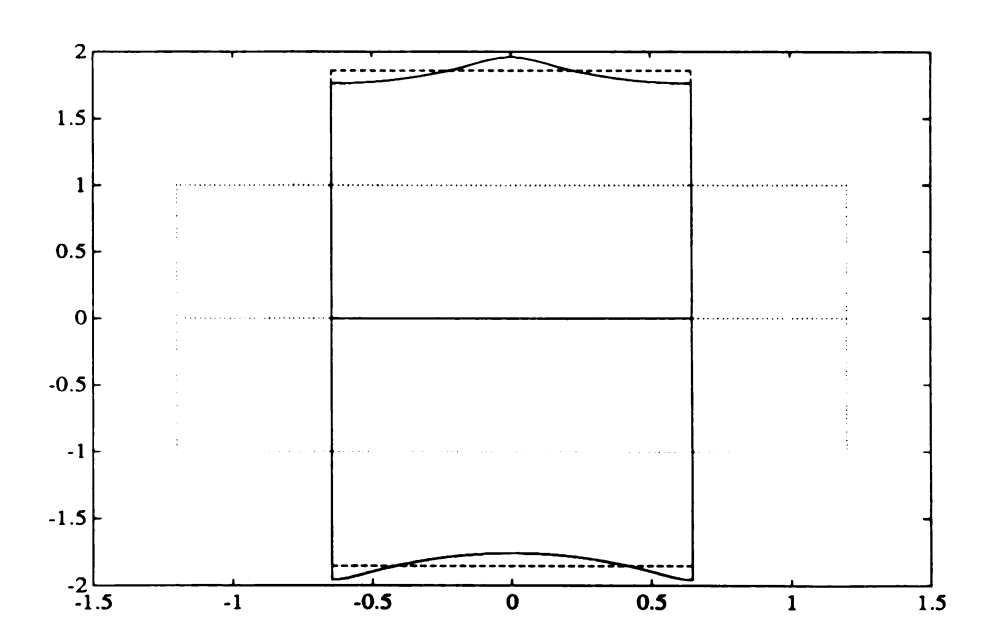


Figure 5.5a. The smooth flexural deformation portion at ϵ =0.0002, m=2, η =5.236, β =3.0, α =0.5, λ = Φ_2 (5.326,3.0,0.5)=3.457. The overall deformation was shown previously in Figure 4.2.

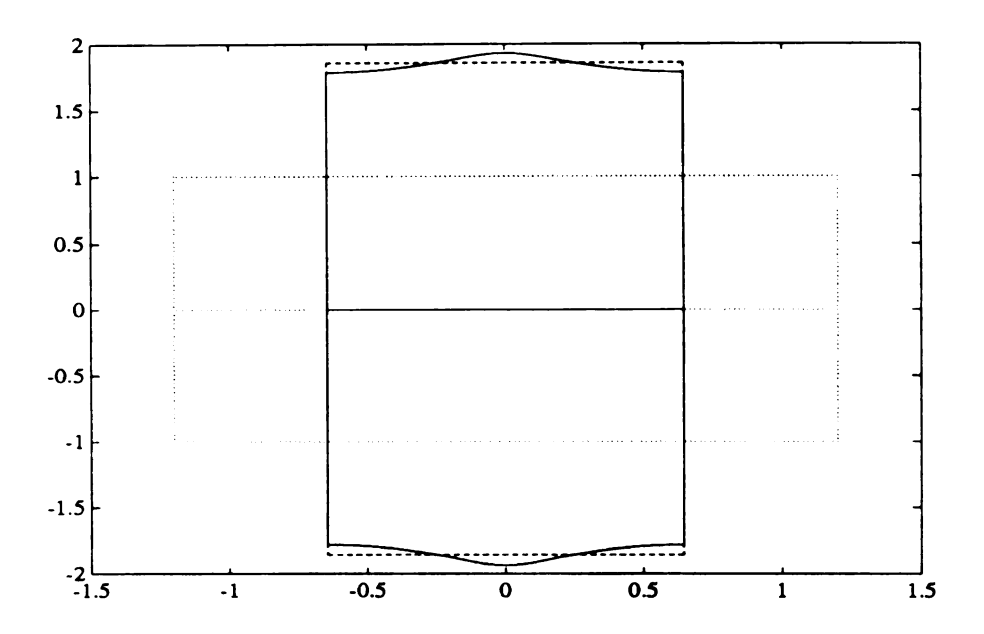


Figure 5.5b. The smooth barrelling deformation portion at ϵ =0.0002, m=2, η =5.236, β =3.0, α =0.5, λ = Φ_2 (5.326,3.0,0.5)=3.457. The overall deformation was shown previously in Figure 4.2.

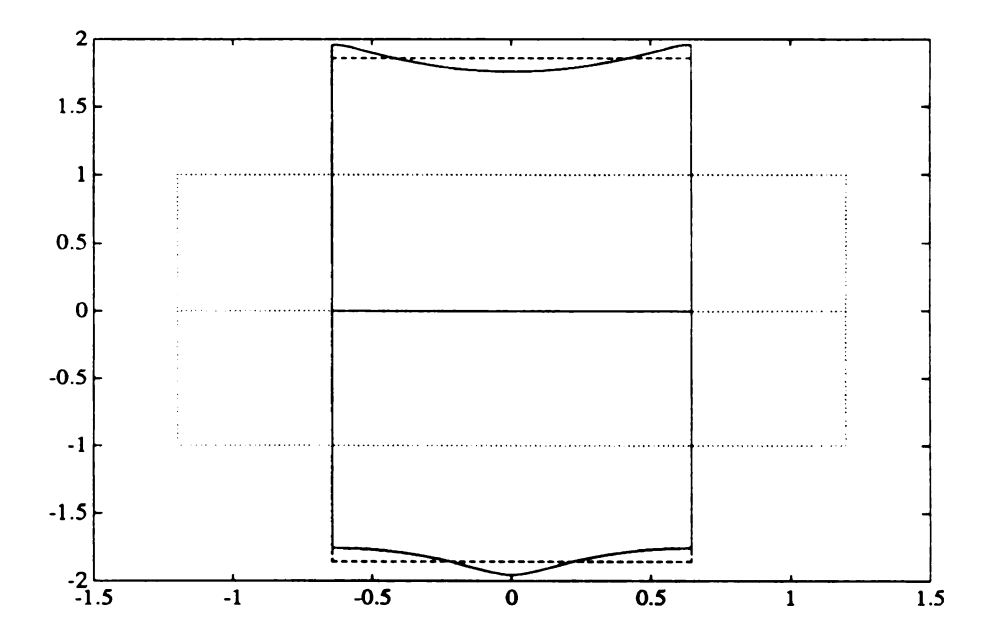


Figure 5.5c. The residual flexural deformation portion at ϵ =0.0002, m=2, η =5.236, β =3.0, α =0.5, λ = Φ_2 (5.236,3.0,0.5)=3.457. The overall deformation was shown previously in Figure 4.2.

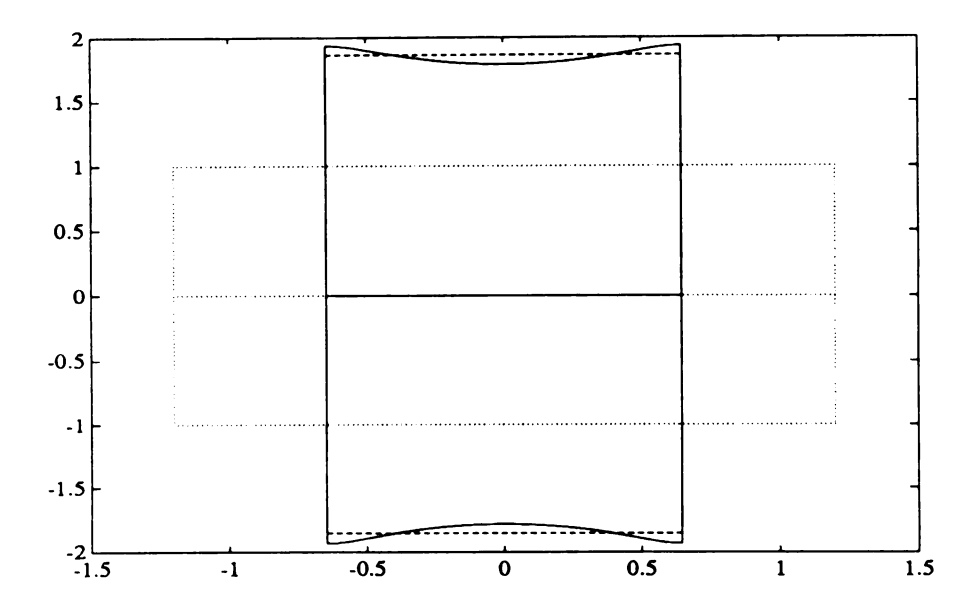


Figure 5.5d. The residual barrelling deformation portion at ϵ =0.0002, m=2, η =5.236, β =3.0, α =0.5, λ = Φ_2 (5.236,3.0,0.5)=3.457. The overall deformation was shown previously in Figure 4.2.

One difficulty in directly comparing the deformations as discussed here to the flexural and barrelling deformations discussed in Sawyers and Rivlin's [3] [4] is due to the choice of origin of the coordinate system. In the context of Sawyers and Rivlin[3] [4] as well as Pence and Song [9] [10], the origin is always chosen so as to lie at the center of the overall plate (and hence in its mid-plane). In contrast, here the origin is chosen to lie on the interfacial plane, which coincides with the midplane only for the case $\alpha=1/2$. It is thus instructive to view the deformations as discussed here in an alternative coordinate system centered at the mid-plane. To do this we introduce the coordinate transformation

$$Y_1 = X_1, Y_2 = X_2 + a, Y_3 = X_3, (5.1)$$

where $-l_2 \le a \le l_2$ is given by

$$a = (2\alpha - 1)1_2. (5.2)$$

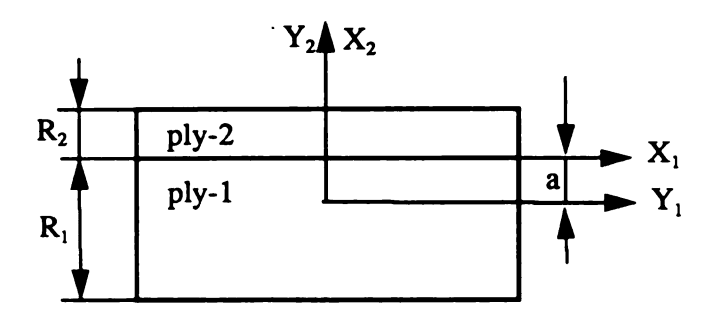


Figure 5.6 Coordinate Transformation

The solution for equation (2.53) becomes V_2 (and correspondingly V_1) with respect to coordinate system Y_1 - Y_2 - Y_3 . By the coordinate transformation defined in (5.1), it is readily seen that

$$V_2(Y_2) = U_2(Y_2 - a) \qquad V_1(Y_2) = U_1(Y_2 - a).$$
 (5.3)

Expressing V₂ in full we have

$$V_{2}(Y_{2}) = P_{1}^{(j)} \cosh(\Omega Y_{2}) + P_{2}^{(j)} \sinh(\Omega Y_{2}) + Q_{1}^{(j)} \cosh(\lambda \Omega Y_{2}) + Q_{2}^{(j)} \sinh(\lambda \Omega Y_{2}),$$
(5.4)

where j = 1, 2, and

$$\begin{split} P_{1}^{(j)} &= L_{1}^{(j)} \cosh \left(\Omega a\right) - L_{2}^{(j)} \sinh \left(\Omega a\right), \\ P_{2}^{(j)} &= L_{2}^{(j)} \cosh \left(\Omega a\right) - L_{1}^{(j)} \sinh \left(\Omega a\right), \\ Q_{1}^{(j)} &= M_{1}^{(j)} \cosh \left(\lambda \Omega a\right) - M_{2}^{(j)} \sinh \left(\lambda \Omega a\right), \\ Q_{2}^{(j)} &= M_{2}^{(j)} \cosh \left(\lambda \Omega a\right) - M_{1}^{(j)} \sinh \left(\lambda \Omega a\right). \end{split}$$
(5.5)

This then gives

$$\begin{split} L_{1}^{(j)} &= P_{1}^{(j)} \cosh \left(\Omega a\right) + P_{2}^{(j)} \sinh \left(\Omega a\right), \\ L_{2}^{(j)} &= P_{2}^{(j)} \cosh \left(\Omega a\right) + P_{1}^{(j)} \sinh \left(\Omega a\right), \\ M_{1}^{(j)} &= Q_{1}^{(j)} \cosh \left(\lambda \Omega a\right) + Q_{2}^{(j)} \sinh \left(\lambda \Omega a\right), \\ M_{2}^{(j)} &= Q_{2}^{(j)} \cosh \left(\lambda \Omega a\right) + Q_{1}^{(j)} \sinh \left(\lambda \Omega a\right). \end{split}$$
(5.6)

Recall from (2.64) that $\beta=1$ is one way to obtain the noncomposite case. However if $\beta=1$ and $\alpha \neq 1/2$ then this noncomposite case is being treated in a nonsymmetric coordinate system for the axis system $X_1-X_2-X_3$. However, the treatment is symmetric in the coordinate system $Y_1-Y_2-Y_3$. If given $\lambda=\Phi_1(\eta,1,\alpha)$, generally in this case [3], [4], [9], [10],

$$P_1^{(1)} = P_1^{(2)} \neq 0, Q_1^{(1)} = Q_1^{(2)} \neq 0,$$

 $P_2^{(1)} = P_2^{(2)} = Q_2^{(1)} = Q_2^{(2)} = 0.$ (5.7)

These P's and Q's in equation (5.7) make $V_2(Y_2)$ a even function. Then the buckling deformations corresponding to $\lambda = \Phi_1(\eta, \beta, \alpha)$ are purely flexural with respect to coordinate system $Y_1 - Y_2 - Y_3$. This is the same result as Sawyers and Rivlin [3] [4] as well as Pence and Song [9] [10] have obtained. On account of (5.6) and (5.7), if $a \neq 0$, (i.e. $\alpha \neq 1/2$ according to (5.5)) but $\beta = 1$, we have

$$L_{1}^{(1)} = L_{1}^{(2)} = P_{1}^{(1)} \cosh(\Omega a) \neq 0,$$

$$L_{2}^{(1)} = L_{2}^{(2)} = P_{1}^{(1)} \sinh(\Omega a) \neq 0,$$

$$M_{1}^{(1)} = M_{1}^{(2)} = Q_{1}^{(1)} \cosh(\lambda \Omega a) \neq 0,$$

$$M_{2}^{(1)} = M_{2}^{(2)} = Q_{1}^{(1)} \sinh(\lambda \Omega a) \neq 0.$$
(5.8)

It can be seen from (5.8) that all eight components of I are nonzero and make U_2 neither an even function of X_2 nor an odd one. Further, by applying the decomposition (4.4) (4.9), we have

$$a_1 = P_1^{(1)} \cosh(\Omega a), \qquad a_3 = Q_1^{(1)} \cosh(\lambda \Omega a), b_2 = P_1^{(1)} \sinh(\Omega a), \qquad b_4 = Q_1^{(1)} \sinh(\lambda \Omega a),$$
 (5.9)

and

$$c_2 = c_4 = d_1 = d_3 = 0,$$
 or $c = d = 0.$ (5.10)

So, even in the noncomposite case, if there is no symmetry in direction of thickness in a reference system $(X_1-X_2-X_3)$ here, there exist both smooth flexural and smooth barrelling deformations. Calculated from (4.10), we have

$$\|\mathbf{I}\|_{2}^{2} = \|\mathbf{a}\|_{2}^{2} + \|\mathbf{b}\|_{2}^{2}, \tag{5.11}$$

where

$$\|\mathbf{a}\|_{2}^{2} = 2 \left\{ \left(P_{1}^{(1)} \cosh \left(\Omega \mathbf{a} \right) \right)^{2} + \left(Q_{1}^{(1)} \cosh \left(\lambda \Omega \mathbf{a} \right) \right)^{2} \right\},$$

$$\|\mathbf{b}\|_{2}^{2} = 2 \left\{ \left(P_{1}^{(1)} \sinh \left(\Omega \mathbf{a} \right) \right)^{2} + \left(Q_{1}^{(1)} \sinh \left(\lambda \Omega \mathbf{a} \right) \right)^{2} \right\}.$$
(5.12)

Since $\Omega = \eta/(2l_2)$ it follows that

$$\frac{\|\mathbf{a}\|_{2}^{2}}{\|\mathbf{I}\|_{2}^{2}} = \begin{cases} 1 & \text{as } \eta \to 0 \\ 1/2 & \text{as } \eta \to \infty \end{cases}, \tag{5.13}$$

and

$$\frac{\|\mathbf{b}\|_{2}^{2}}{\|\mathbf{I}\|_{2}^{2}} = \begin{cases} 0 & \text{as } \eta \to 0 \\ 1/2 & \text{as } \eta \to \infty \end{cases}, \tag{5.14}$$

for the first root λ - η curve λ = $\Phi_1(\eta,1,\alpha)$ with $\alpha \neq 1/2$.

If given $\lambda = \Phi_2(\eta, \beta, \alpha)$ for this noncomposite case ($\beta = 1$ and $\alpha \neq 1/2$), we have

$$P_{2}^{(1)} = P_{2}^{(2)} \neq 0, \qquad Q_{2}^{(1)} = Q_{2}^{(2)} \neq 0,$$

$$P_{1}^{(1)} = P_{1}^{(2)} = Q_{1}^{(1)} = Q_{1}^{(2)} = 0,$$
(5.15)

in general. In this instance, these P's and Q's in equation (5.15) make $V_2(Y_2)$ an odd function. The buckling deformations corresponding to $\lambda = \Phi_2(\eta, \beta, \alpha)$ are, therefore, purely barrelling with respect to coordinate system $Y_1 - Y_2 - Y_3$. This again is the same result as in [3] [4] or [9] [10]. Similar to the discussion made above, the eight components of I are nonzero and give rise to both smooth flexural and smooth barrelling deformations and restrain the residual flexural deformation c as well as residual barrelling deformation d, with reference to $X_1 - X_2 - X_3$. Analogous to (5.13) (5.14) we have

$$\frac{\|\mathbf{a}\|_{2}^{2}}{\|\mathbf{I}\|_{2}^{2}} = \begin{cases} 0 & \text{as } \eta \to 0 \\ 1/2 & \text{as } \eta \to \infty \end{cases}, \tag{5.16}$$

as well as

$$\frac{\|\mathbf{b}\|_{2}^{2}}{\|\mathbf{I}\|_{2}^{2}} = \begin{cases} 1 & \text{as } \eta \to 0 \\ 1/2 & \text{as } \eta \to \infty \end{cases}$$
 (5.17)

for the second root $\lambda-\eta$ curve $\lambda=\Phi_2(\eta,1,\alpha)$ with $\alpha\neq 1/2$. Finally recall for the case $\beta=1$ that the third root $\lambda-\eta$ curve $\lambda=\Phi_3(\eta,1,\alpha)$ has moved up to infinity and hence does not exist.

In this thesis we have studied the buckling of the 2-ply nonlinear elastic plate, formulated and solved the problem, fulfilled the procedure for predicting the buckling loads, and studied the deformation modes. In comparison to the symmetric 3-ply problem extensively studied by Pence and Song [9] [10] as well as Kim [13], the 2-ply buckling problem of the composite plate gives one additional family of buckling stretch $(\Phi_3(\eta,\beta,\alpha))$ to the noncomposite cases whereas in the symmetric 3-ply problem there are two additional families of buckling stretches. Instead of the pure flexural and pure barrelling deformation modes in the symmetric 3-ply problem, the buckling deformations of the 2-ply problem are in mixed modes having both flexural and barrelling characters.

LIST OF REFERENCES

- [1] R. W. Ogden, Non-linear elastic deformations. Halsted Press, New York, 1984.
- [2] M. A. Biot, <u>Mechanics of Incremental Deformations</u>. John Wiley & Sons, New York, 1965.
- [3] K. N. Sawyers and R. S. Rivlin, "Bifurcation conditions for a thick elastic plate under thrust". Int. J. Solids Structures, Vol. 10, pp. 483-501, 1974.
- [4] K. N. Sawyers and R. S. Rivlin, "Stability of a thick elastic plate under thrust". Journal of Elasticity, Vol. 12, No. 1, January 1982.
- [5] P. J. Davies, "Buckling and barrelling instabilities in finite elasticity". Journal of Elasticity, Vol. 21, pp. 147-192, 1989.
- [6] I. W. Burgess and M. Levinson, "The instability of slightly compressible rectangular rubberlike solids under bixial loading". Int. J. Solids Structures, Vol. 8, pp. 133-148, 1972.
- [7] B. Budiansky, "Theory of buckling and post-buckling behavior of elastic structures". in Advances of Applied Mechanics, 14, pp. 1-65, 1974, ed. C. S. Yih, Academic Press.
- [8] M. A. Biot, "Edge Buckling of a laminated medium". Int. J. Solids Structures, Vol. 4, pp. 125-137, 1968.

- [9] T. J. Pence and J. Song, "Buckling instabilities in highly deformable composite laminate plates". Proceedings of the American Society for Composites Fifth Technical Congress, pp. 459-468, 1990.
- [10] T. J. Pence and J. Song, "Buckling instabilities in a thick elastic three ply composite plate under thrust". Int. J. Solids Structures, Vol. 27, pp. 1809-1828, 1991.
- [11] G. M. Phillips, P. J. Taylor, <u>Theory and Applications of Numerical Analysis</u>. Academic Press, 1973.
- [12] M. Avriel, Nonlinear Programming: Analysis and Methods. Prentice-Hall, 1976.
- [13] Sang Woo Kim, Research in progress.

APPENDIX

THE EXPRESSION OF $\Psi(\lambda, \eta, \beta, \alpha)$

 $\Psi(\lambda,\eta,\beta,\alpha)$ can be expressed as

$$\Psi(\lambda, \eta, \beta, \alpha) = \frac{1}{16} \Lambda^T \mathbf{P}^T \mathbf{E}, \qquad (A.1)$$

where

$$\Lambda = \{\lambda^{-6}, \lambda^{-5}, ..., \lambda^{0}, ..., \lambda^{6}, \lambda^{7}\}^{T}, \tag{A.2}$$

$$\mathbf{E} = \{e^{\eta \kappa_{-12}}, e^{\eta \kappa_{-11}}, ..., e^{\eta \kappa_{0}}, ..., e^{\eta \kappa_{11}}, e^{\eta \kappa_{12}}\}^{T}, \tag{A.3}$$

and P is a 25 by 14 matrix with entries $P_{i,j}(\beta)$

$$\mathbf{P} = (P_{i,j}(\beta))_{25 \times 14}. \tag{A.4}$$

The $\kappa_i^{}=\kappa_i^{}(\lambda,\alpha)$ (i=-12, ... ,12) are given by

$$\kappa_0 = 0, \tag{A.5}$$

$$\kappa_{1} = (\lambda + 1), \qquad \kappa_{-1} = -(\lambda + 1),
\kappa_{2} = (\lambda + 2\alpha - 1), \qquad \kappa_{-2} = -(\lambda + 2\alpha - 1),
\kappa_{3} = (\lambda - 2\alpha + 1), \qquad \kappa_{-3} = -(\lambda - 2\alpha + 1),
\kappa_{4} = (\lambda - 1), \qquad \kappa_{-4} = -(\lambda - 1),
\kappa_{5} = (2\alpha\lambda - \lambda + 1), \qquad \kappa_{-5} = -(2\alpha\lambda - \lambda + 1),
\kappa_{6} = (\lambda + 1)(2\alpha - 1), \qquad \kappa_{-6} = -(\lambda + 1)(2\alpha - 1),
\kappa_{7} = (\lambda - 1)(2\alpha - 1), \qquad \kappa_{7} = -(\lambda - 1)(2\alpha - 1),$$

$$\begin{split} \kappa_8 &= \; (2\alpha\lambda - \lambda - 1) \,, & \kappa_{-8} &= \; -(2\alpha\lambda - \lambda - 1) \,, \\ \kappa_9 &= \; (\lambda + 1) \,\alpha, & \kappa_{-9} &= \; -(\lambda + 1) \,\alpha, \\ \kappa_{10} &= \; (\lambda - 1) \,\alpha, & \kappa_{-10} &= \; -(\lambda - 1) \,\alpha, \\ \kappa_{11} &= \; (\lambda + 1) \; (1 - \alpha) \,, & \kappa_{-11} &= \; -(\lambda + 1) \; (1 - \alpha) \,, \\ \kappa_{12} &= \; (\lambda - 1) \; (1 - \alpha) \,, & \kappa_{-12} &= \; -(\lambda - 1) \; (1 - \alpha) \,. \end{split}$$

One finds that the 350 $P_{i,j}(\beta)$'s are constrained by the following relation:

$$P_{i,j} = P_{-i,j}, \quad i = 1, 2, ..., 12, \quad j = -6, -5, ..., 0, ..., 6, 7.$$
 (A.6)

The particular values for the $P_{i,j}(\beta)$'s are given in Table A.1 (the distinctive $P_{i,j}(\beta)$'s are denoted by *). The 31 distinctive $P_{i,j}(\beta)$'s are:

$$P_{0,-3} = -128\beta, \tag{A.7}$$

$$P_{0,1} = 1536\beta^2 - 2816\beta + 1536,$$
 (A.8)

$$P_{0.5} = 512\beta^2 - 1152\beta + 512, \tag{A.9}$$

$$P_{2-6} = \beta^2 - 1, \tag{A.10}$$

$$P_{4,-6} = \beta^2 + 2\beta + 1, \tag{A.11}$$

$$P_{4,-4} = 6\beta^2 - 4\beta + 6, \tag{A.12}$$

$$P_{4,-3} = 18\beta^2 - 4\beta + 18, \tag{A.13}$$

$$P_{4-2} = 27\beta^2 - 58\beta + 27, \tag{A.14}$$

$$P_{4,0} = 116\beta^2 - 184\beta + 116, \tag{A.15}$$

$$P_{4,1} = 140\beta^2 - 344\beta + 140, \tag{A.16}$$

$$P_{4,2} = 183\beta^2 - 498\beta + 183, \tag{A.17}$$

$$P_{4,4} = 166\beta^2 - 260\beta + 166, \tag{A.18}$$

$$P_{4.5} = 66\beta^2 - 100\beta + 66, \tag{A.19}$$

$$P_{4,6} = 13\beta^2 - 22\beta + 13, \tag{A.20}$$

$$P_{4,7} = \beta^2 - 2\beta + 1, \tag{A.21}$$

$$P_{9,-4} = -16\beta + 16, \tag{A.22}$$

$$P_{9,-2} = 32\beta^2 - 112\beta + 80, \tag{A.23}$$

$$P_{9.0} = 256\beta^2 - 416\beta + 160, \tag{A.24}$$

$$P_{9,1} = -320\beta^2 + 704\beta - 384, \tag{A.25}$$

$$P_{9,2} = 448\beta^2 - 864\beta + 416,$$
 (A.26)

$$P_{9,4} = 256\beta^2 - 592\beta + 336, \tag{A.27}$$

$$P_{9,5} = -160\beta^2 + 288\beta - 128, \tag{A.28}$$

$$P_{9,6} = 32\beta^2 - 48\beta + 16, \tag{A.29}$$

$$P_{11,-4} = 16\beta^2 - 16\beta \tag{A.30}$$

$$P_{11,-2} = 80\beta^2 - 112\beta + 32, \tag{A.31}$$

$$P_{11,0} = 160\beta^2 - 416\beta + 256, \tag{A.32}$$

$$P_{11,1} = -384\beta^2 + 704\beta - 320, \tag{A.33}$$

$$P_{11, 2} = 416\beta^2 - 864\beta + 448, \tag{A.34}$$

$$P_{11, 4} = 336\beta^2 - 592\beta + 256, \tag{A.35}$$

$$P_{11.5} = -128\beta^2 + 288\beta - 160, \tag{A.36}$$

$$P_{11.6} = 16\beta^2 - 48\beta + 32. \tag{A.37}$$

		T					
i		-5	-4	-3	-2	-1	0
0	0	0	0	*	0	512P _{4,7}	0
1	-P _{4,-6}	P _{4,7}	-P _{4,-4}	P _{4,-3}	-P _{4,-2}	63P _{4,7}	-P _{4,0}
2	*	-P _{4,7}	6P _{2,-4}	-2P _{4,7}	11P _{2,-6}	P _{4,7}	-12P _{2,-6}
3	-P _{2,-6}	-P _{4,7}	-6P _{2,-4}	-2P _{4,7}	-11P _{2,-6}	P _{4,7}	12P _{2,-6}
4	*	P _{4,7}	*	*	*	63P _{4,7}	*
5	P _{2,-6}	-P _{4,7}	6P _{2,4}	-2P _{4,7}	11P _{2,-6}	P _{4,7}	-12P _{2,-6}
6	-P _{4,7}	P _{4,7}	-6P _{4,7}	18P _{4,7}	-27P _{4,7}	63P _{4,7}	-116P _{4.7}
7	P _{4,7}	P _{4,7}	6P _{4,7}	18P _{4,7}	27P _{4,7}	63P _{4,7}	116P _{4,7}
8	-P _{2,-6}	-P _{4,7}	-6P _{2,-4}	-2P _{4,7}	-11P _{2,-6}	P _{4,7}	12P _{2,-6}
9	0	0	*	-2P _{11,-4}	*	-128P _{4,7}	*
10	0	0	-P _{9,-4}	-2P _{11,-4}	-P _{9,-2}	-128P _{4,7}	-P _{9,-0}
11	0	0	*	-2P _{9,-4}	*	-128P _{4,7}	*
12	0	0	-P _{11,-4}	-2P _{9,-4}	-P _{11,-2}	-128P _{4,7}	-P _{11,0}
; i	1	1 2	T 2	Γ .	<u> </u>		
1 3		2	3	4	5	6	7
0	*	0	1536P _{4,7}	0	*	0	0
1	P _{4,1}	-P _{4,2}	223P _{4,7}	-P _{4,4}	P _{4,5}	-P _{4,6}	P _{4,7}
2	20P _{4,7}	-41P _{2,-6}	-31P _{4,7}	38P _{2,-6}	14P _{4,7}	-3P _{2,-6}	-P _{4,7}
3	20P _{4,7}	41P _{2,-6}	-31P _{4,7}	-38P _{2,-6}	14P _{4,7}	3P _{2,-6}	-P _{4,7}
4	*	*	223P _{4,7}	*	*	*	*
5	20P _{4,7}	-41P _{2,-6}	-31P _{4,7}	38P _{2,-6}	14P _{4,7}	-3P _{2,-6}	-P _{4,7}
6	1400	1000					
	140P _{4,7}	-183P _{4,7}	223P _{4,7}	-166P _{4,7}	66P _{4.7}	-13P ₄₇	P_{47}
7	140P _{4,7}	183P _{4,7}	223P _{4,7} 223P _{4,7}	-166P _{4,7}	66P _{4,7}	-13P _{4,7}	P _{4,7}
	140P _{4,7} 140P _{4,7} 20P _{4,7}	183P _{4,7}	223P _{4,7}	166P _{4,7}	66P _{4,7}	13P _{4,7}	P _{4,7}
7	140P _{4,7} 20P _{4,7} *		223P _{4,7} -31P _{4,7}				P _{4,7} -P _{4,7}
7 8	140P _{4,7} 20P _{4,7}	183P _{4,7} 41P _{2,-6} *	223P _{4,7} -31P _{4,7} -384P _{4,7}	166P _{4,7} -38P _{2,-6} *	66P _{4,7} 14P _{4,7} *	13P _{4,7} 3P _{2,6}	P _{4,7} -P _{4,7} 0
7 8 9	140P _{4,7} 20P _{4,7} *	183P _{4,7} 41P _{2,-6}	223P _{4,7} -31P _{4,7} -384P _{4,7} -384P _{4,7}	166P _{4,7} -38P _{2,-6}	66P _{4,7} 14P _{4,7}	13P _{4,7} 3P _{2,-6}	P _{4,7} -P _{4,7} 0 0
7 8 9 10	140P _{4,7} 20P _{4,7} * P _{9,1}	183P _{4,7} 41P _{2,-6} * -P _{9,2}	223P _{4,7} -31P _{4,7} -384P _{4,7}	166P _{4,7} -38P _{2,-6} * -P _{9,4}	66P _{4,7} 14P _{4,7} * P _{9,5}	13P _{4,7} 3P _{2,-6} * -P _{9,6}	P _{4,7} -P _{4,7} 0

Table A.1

A calculation finds that

$$\sum_{i=-12}^{12} P_{i,j}(\beta) = 0 \qquad j = -6, -5, ..., 7.$$
(A.38)

Alternatively, $\Psi(\lambda,\eta,\beta,\alpha)$ can be expressed as

$$\Psi(\lambda, \eta, \beta, \alpha) = \frac{1}{8} \Lambda^T \tilde{\mathbf{P}}^T \mathbf{H}, \qquad (A.39)$$

where L is again given by (A.2) and

$$\mathbf{H} = \left\{ \cosh\left(\eta \kappa_{0}\right), \cosh\left(\eta \kappa_{1}\right), ..., \cosh\left(\eta \kappa_{12}\right) \right\}^{T}. \tag{A.40}$$

And $\tilde{\textbf{P}}$ is a matrix of 13 × 14 with entries $\tilde{P}_{i,\,j}\left(\beta\right)$, i=0,1, ..., 12, j=-6,-5, ..., 0, ..., 6,7:

$$\tilde{\mathbf{P}} = (\tilde{\mathbf{P}}_{i,j}(\boldsymbol{\beta}))_{13 \times 14}, \tag{A.41}$$

where

$$\tilde{P}_{i,j} = P_{i,j}$$
 $i = 1, ..., 12, j = -6, ..., 7,$ (A.42)

$$\tilde{P}_{0,j} = \frac{1}{2} P_{0,j}$$
 $j = -6, ..., 7.$ (A.43)

